

Scientific Spokesman

K. Wendell Chen  
Department of Physics  
Michigan State University  
E. Lansing, Michigan 48823  
FTS Direct (517) 353-5459

A Detailed Study of "Extra Muon" Production in Deep Inelastic  
Muon Interactions

B. Ball, D. Bauer, C. Chang, K. W. Chen, S. Hansen, L. Litt, J. Kiley,  
A. Kotlewski and P. F. Schewe

Michigan State University  
East Lansing, Michigan 48824

January 23, 1976

### Abstract

"A Detailed Study of 'Extra Muon' Production in Deep Inelastic Muon Interactions"

B. Ball, D. Bauer, C. Chang, K. W. Chen, S. Hansen, L. Litt, J. Kiley, A. Kotlewski and P. F. Schewe

We propose here a specific missing energy measurement in direct muon production by high energy muons. First we briefly summarize heretofore unpublished dimuon data collected in a previous muon scattering experiment (E-26). These data support a possible new particle production mechanism. Forty events were found to show extra muons accompanying the scattered muon. These extra muon(s) could conceivably be interpreted as the leptonic or semileptonic decays of some new hadron(s) produced in high momentum-transfer muon interactions. The rate for the extra muon production is greater than  $2 \times 10^{-3}$  of single  $\mu$  events.

The proposed experiment will be performed using the E319 apparatus, consisting of a newly constructed fine-grained hadron calorimeter (240" in length and 1 7/8" Fe sandwiched by 1/4" plastic scintillators), an improved muon spectrometer and new beam proportional chambers to be shared with the E398 group. This new apparatus is particularly well suited to observe the production and weak decays of new hadrons. Among the unique advantages in the detail studies of muon-production of new particles include 1) a precise knowledge of kinematics: incoming muon energy,  $E_0$ ,

scattered muon energy  $E'$ ,  $Q^2$ ,  $\nu$ ,  $x$ , and  $W$ , etc., 2) a good measurement of missing energy carried by neutrinos, 3) a large solid angle acceptance for final state muons, 4) an experimental verification of "promptness" of extra muon yields using varying target densities and 5) flexibility in trigger with three sets of new trigger counter hodoscopes.

A run of  $10^{11}$  muons is requested at  $E_\mu = 300$  GeV with an intensity of  $10^6$  muons/pulse. This run can be carried out in the same quadrupole-triplet running period as E319 following data taking by E398. We anticipate collecting 2300 dimuon events.

We emphasize here that our improved apparatus resembles that proposed in proposal E-225 (1973), in which the original idea of using a target-calorimeter to study high momentum-transfer interactions was advanced for the first time. The fact that we were able to observe dimuon events with high efficiency using E26 apparatus demonstrates that our apparatus will be more than adequate to search for the existence and to study the weak decay of new particles.

## TABLE OF CONTENTS

	Page
I      Introduction	1
II     Deep Inelastic Muoproduction	2
III    Possible Origin of Multimuon Events	9
IV     Apparatus For Further Study of Dimuon and Trimuons	11
V      Event Rate	13
VI     Running Time and Scenerio For This Exposure	15
VII    NAL Contributions	16
References	16

## I. Introduction

A run of  $10^{11}$  muons during the next triplet trainload running period is proposed to investigate in greater detail and precision, possible evidence for new particle production in a previous muon scattering experiment (E26). In the following sections we briefly describe characteristics of 32 events which exhibit the presence of an extra muon along with the scattered muon.

The processes giving rise to an extra muon in the final state

$$\begin{aligned}\mu^+ + N &\rightarrow \mu^+ + \mu^- + \text{hadrons} \\ &\rightarrow \mu^+ + \mu^+ + \text{hadrons}\end{aligned}\tag{1}$$

and

$$\begin{aligned}\mu^- + N &\rightarrow \mu^- + \mu^+ + \text{hadrons} \\ &\rightarrow \mu^- + \mu^- + \text{hadrons}\end{aligned}\tag{2}$$

have been observed at the rate exceeding  $2 \times 10^{-3}$  per deep inelastic muon scattering event ( $E' > 30$  GeV and  $\theta > 17$  mrad).

Six events with three muons in the final state,

$$\begin{aligned}\mu^+ + N &\rightarrow \mu^+ + \mu^+ + \mu^- + \text{hadrons} \\ \mu^- + N &\rightarrow \mu^- + \mu^- + \mu^+ + \text{hadrons}\end{aligned}\tag{3}$$
$$\tag{4}$$

have also been observed at the rate exceeding  $4 \times 10^{-4}$  per deep inelastic muon scattering event defined above.

The analyses of these events are not yet final, but current conclusions should justify a more detailed experimental investigation

of the relevant physics at the earliest moment using a functional apparatus.

The proposed experimental apparatus is the one to be used in E319, an experiment to further test scaling beyond the kinematical region covered in E-26<sup>1,2</sup>.

The detector is now well suited to study muon pairs or triplets as it provides:

- 1) Identification of neutrinos in final state by observing the "missing energy" using the calorimeter and E' measurement.
- 2) Observation of large solid angle (up to  $\pm 18^\circ$  in lab) of muons with good identification.
- 3) Measurement of momentum to  $\pm 10\%$  of final state muons within 250 mrad.
- 4) Energy measurement of hadrons to  $\leq 15\%$ .
- 5) Flexible triggering using road-map counters.
- 6) Variable target density ( $\text{CH}_2$ , Al, Fe)

A run at the conclusion of E398 run late this summer using the triplet trainload is envisioned. All the target materials are on hand so that measurements can commence without delay. This measurement will be the last one using the muon scattering apparatus (E26/E319) we have laboriously constructed during the past few years. Based on the measured yield of events with extra muons, we anticipate collecting  $\geq 2300$  events which may well be positively identified as weak decays of new hadrons.

## II. Data On Deep Inelastic Muoproduction of Extra Muons

### 1. E-26 Data Sample

In the data sample we used to test scaling (E26), approximately

40 multimMuon events of great interest were found. Thirty-two dimuon events show clearly an extra muon originating from the target vertex and penetrate the entire apparatus. Typical events are shown in Figure 1-7. An event showing all three muons penetrating the E26 apparatus as shown in Figure 8. Six events of this type were found.

The muon beam was derived from a simple quadrupole triplet tuned for 150 GeV charge hadrons. The primary proton energy was 300 GeV. The trigger requirement for all events was a single muon which penetrated the entire E26 apparatus ( $E_\mu > 11\text{GeV}$ ). ("Long Target" configuration). A crude instrumented-target was used to identify the presence of electromagnetic or hadron cascade showers.

We looked for multimMuon events only in data runs with both  $\mu^+$  and  $\mu^-$  exposures in order to study the charge asymmetry of production processes.

An event is considered a candidate by the following criteria:

1. Dimuons must penetrate all eight magnets:  $E_\mu > 11\text{ GeV}$ .
2. Trajectories extrapolate to the target to within  $\Delta \leq 5\text{ cm}$ .
3. Angular acceptance  $17\text{ mrad} < \theta_\mu < 250\text{ mrad}$ .
4. Correct timing and hodoscope information.

After the candidates were found, further scanning and measurements were made by physicists. In this exposure,  $5.25 \times 10^9$  muons were allowed to traverse 72" of Fe target at  $E_\mu = 150\text{ GeV}$ . Table I summarizes the result of the event finding analysis:

TABLE I

Total accepted single muon events (with $E' > 30$ )	13962
Multimuon candidates found by VØREPAIR Scan	1400
Good pairs found after scanning and measurement	32
Good tridents found after scanning and measurement	6

## 2. Branching Ratio

Uncorrected branching ratio is easily calculated:

$$\frac{\sigma(\mu N \rightarrow \mu\mu X)}{\sigma(\mu N \rightarrow \mu' X)} = \frac{32}{13962} = 2.4 \times 10^{-3} \quad (5)$$

and

$$\frac{\sigma(\mu N \rightarrow \mu\mu\mu X)}{\sigma(\mu N \rightarrow \mu' X)} = \frac{6}{13962} = 4 \times 10^{-4}$$

These values must be corrected for geometric detection efficiency since both tracks from an event must pass through the entire spectrometer. This correction is yet to be finalized by a Monte-Carlo calculation.

## 3. Charge Asymmetry in Multimuon Production

$\mu^- \mu^+, \mu^+ \mu^-, \mu^+ \mu^+, \mu^- \mu^-$  and  $\mu\mu\mu$  events found are classified as "opposite-sign-pairs" (OSP), "same-sign-pairs" (SSP), and trimuons (TM), respectively as shown below.

	$\mu^+$ Incident	Number of Events
OSP	$\mu^+ \rightarrow \mu^+ \mu^-$	10
SSP	$\mu^+ \rightarrow \mu^+ \mu^+$	8
TM	$\mu^+ \rightarrow \mu^+ \mu^+ \mu^-$	2



	<u><math>\mu^-</math> Incident</u>	<u>Number of Events</u>
OSP	$\mu^- \rightarrow \mu^+ \mu^-$	6
SSP	$\mu^- \rightarrow \mu^- \mu^-$	9
TM	$\mu^- \rightarrow \mu^- \mu^- \mu^+$	4

The charge asymmetry A, after combining both  $\mu^+$  and  $\mu^-$  data, is

$$A = \frac{\text{No. of opposite sign pairs}}{\text{No. of same sign pairs}} = \frac{16}{17} = 0.94 \pm 0.20$$

Within statistics, no charge asymmetry in muoproduction is observed.

#### 4. Energy Distribution of Extra Muons

Only opposite-sign-pairs (OSP:  $\mu^+ \mu^-$  and  $\mu^- \mu^+$ ) are used to study the energy distributions of the produced muon  $p_2$ .  $p_1$  is the scattered muon momentum. Fig. 7 shows that  $p_1 > p_2$ , suggesting a leading particle effect.

This feature may help us identify  $p_1$  and  $p_2$  for SSP's.

#### 5. $\langle Q^2 \rangle$ , x, W and $M_{\mu\mu}$

Figure 10 shows the  $Q^2$  distribution for the OSP's.

Figure 11 shows x distribution for 16 OSP's. We note that  $x < 0.05$ , or  $\omega \geq 10$ .

This is in the same region where some scaling violations are found.<sup>2</sup>

The missing mass of the virtual photon-nucleon system, W, is shown in Figure 12. There seems to be a cutoff at  $W \sim 10$  GeV. The W distribution for single  $\mu$  events is also shown. Values of W for pairs are in general higher than deep inelastic events.

If the muon pairs are direct decays of a massive object, then  $M_{\mu\mu}^2 = (p_1 + p_2)^2$ , the (invariant mass)<sup>2</sup> should show a peak. Figure 13

shows the  $M_{\mu\mu}$  distribution. There is no evidence of a peak in the  $M_{\mu\mu}$  spectrum.

#### 6. Transverse Momentum, $p_T$ , of the Extra Muon

In muon scattering, the virtual photon defines direction from which transverse momenta of particles can be measured. For comparison in  $\nu$  scattering, on the other hand, a lack of information on the incident  $\nu$  energy does not permit a good measure of direction of hadron jet.

Figure 14 shows the  $p_T$  (relative to virtual photon direction) for 16 OSP's in E26. Figure 15 shows the  $p_T$  distribution for the slow muon of 17 SSP's.

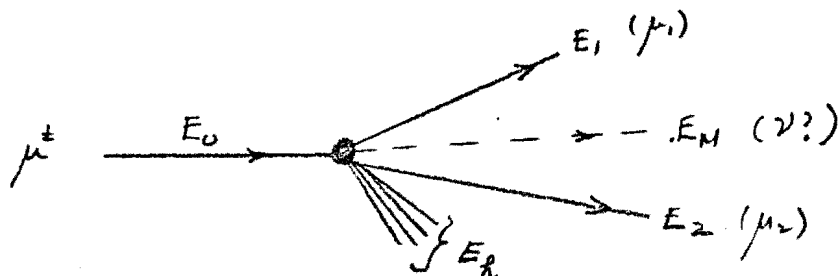
For decays of  $\pi$ 's or K's one expects a distribution  $e^{-6p_T}$  around direction of virtual photon. The observed  $p_T$  distribution is almost flat. The low  $p_T$  region is sensitive to the finite size muon beam and inner aperture in the toroid. This effect is being calculated. Figure 16 shows  $p_T$  distributions for  $\nu$  induced pairs (HPW, 1975)<sup>3</sup> for comparison. Figure 17 shows the momentum of the extra muon versus  $p_T$  for OSP's.

#### 7. $\theta_{\mu\mu}$ , $\Delta\phi_{\mu\mu}$

The opening angle between dimuons is important in that it will help us to estimate the extent of possible contamination due to pure electromagnetic processes. For QED trident production,  $\theta_{\mu\mu}$  should peak at small angles, which is not favored, as shown in Figure 18.  $\langle\theta_{\mu\mu}\rangle$  is 82.6 mrad. The azimuthal angles between the pairs,  $\Delta\phi_{\mu\mu}$ , are shown in Fig. 19.

## 8. Missing Energy Measurement

It is important to measure any missing energy carried away by particles say,  $\nu$  or  $\mu$ , not detected by the apparatus. (See sketch below.)



clearly  $E_0 = E_1 + E_2 + E_h + E_M$

or  $E_M = E_0 - E_1 - E_2 - E_h$

If new hadrons can be produced electromagnetically at large  $Q^2$ , muon experiments are intrinsically superior to  $\nu$  experiments since one can in principle determine the missing energy completely. In a  $\nu$  experiment, the incident  $\nu$  energy is not well defined as well as  $\mu$  experiments even with an improved "dichromatic"  $\nu$  beam.

In E26, the target counters were not operated to measure the energy of cascade showers. The 12" x 12" target counters sandwiched between 4" Fe plates were too small to contain all secondaries. As a result a precise measurement of  $E_h$  was not possible. However, crude information on pulse heights were available. Nearly all the events we observed were accompanied by the existence of a high energy shower.

To summarize, the main features of our dimuon events prior to efficiency corrections (E26) are:

- i) Leading particle effects for opposite sign pairs, i.e.,  
 $p_1 > p_2$
- ii) No measurable charge asymmetry between OSP's and SSP's
- iii) Cutoff of 10 GeV in the missing mass
- iv) "flat"  $p_T$  distribution up to 2.4 GeV/c
- v) No visible peak in apparent  $M_{\mu\mu}$  mass
- vi) Generally large  $Q^2$  ( $\sim 10 \text{ GeV}^2/c^2$ ) and large  $\omega$  ( $\omega \geq 10$ ).  
 $x < 0.05$ . This coincides with where excess events were found.
- vii) High visible hadron inelasticity.
- viii) The uncorrected branching ratio for dimuons to single-muon is  $2 \times 10^{-3}$ . A correction of the order of 2-3 expected. This value is strikingly similar to that observed by the E1A group.

Unique features from our data compared to E1A are items ii), no charge asymmetry; item iii), large W and vi), precise determination of x for dimuon events.

### III. Possible Origin of MultimMuon Events

It is tempting to speculate that our events are due to some new particle production since conventional processes such as,

- i)  $\pi$  or K decay is not favored due to observed large  $p_T$  and large values of  $p_2$ .
- ii) E.m. trident production gives small opening angle pairs and small  $p_T$ , also inelasticity should be small for coherent production.  
Inelastic tridents incoherently produced ( $\sim Z$ ) are also not favored due to small opening angles and low rate at large  $p_T$  caused by a suppression factor  $\sim \left(\frac{p_T}{2M_\mu}\right)^2$
- iii) Production and decay of vector mesons, neutral boson ( $W^0 \rightarrow \mu^+ + \mu^-$ ) are not favored since we see no visible peak in  $M_{\mu\mu}$  distribution.
- iv) Production of  $W \rightarrow \mu^\pm + \nu$ . This is not favored because of the large inelasticity and the relatively small  $p_T$  cutoff observed. Also one would expect  $p_2 > p_1$ .
- v) Particles decaying into  $\mu^+ \mu^-$  (plus scattered  $\mu$ ) with one of the  $\mu$ 's missing detection at large angles is not favored since the efficiency of detecting the third muon (with front large chambers) should give greater than 25 trimuon events. Only 6 are seen.

It is therefore our conjecture that new particle(s) might be produced in deep inelastic muon collisions. This conjecture is reinforced by the following observed and intuitive considerations:

- i) The events at large  $Q^2$  ( $>5$ ) distinguish themselves from the "soft" processes that prevail in conventional hadronic and electromagnetic interactions: heavy objects cannot be easily produced in such processes.
- ii) Virtual or real photons can produce particles that are not already present as target constituents. A good example is the photoproduction of  $\psi/J$  in E87A.
- iii) A direct comparison of the absolute yields in single muon deep inelastic scattering (E26) from those expected from the SLAC data show a 15% excess of events at large values of  $\omega$  ( $\omega > 10$ ). (Figure 20) This is the same  $\omega$  region where our extra muons are found.

Combining our tentative experimental observation and our published results on scaling, we infer that high  $W$  (or  $\nu$ ) events may be due to our exciting new degrees of hadronic freedom in deep inelastic collisions. If the mass of the new hadron is  $m_c$ , the threshold for excitation occurs at  $W_{th}^2 = (2m_c m_N)^2$  and  $q_{th}^2 = n m_c^2$ , where  $n$  is a model dependent quantity of order 1. Near the  $q^2$ - threshold the new hadron production cross-section should be nearly flat, where conventional vector meson production cross-section is already dropping rapidly. Naturally one expects to have an enrichment

factor at least of the order of  $\left(\frac{M_c}{M_p}\right)^2 \approx 10$ .

While these observations are exciting we strongly feel that a better and a larger statistics sample are needed to further explain our effect. We hope that a missing energy measurement will be decisive to exclude all other conventional processes and to prove the existence of new particles by examining the energy balance in their weak decay process.

#### IV. Apparatus for Further Study of Dimuon and Trimuons

We would like to perform this experiment in the same location as Experiment 319. No new equipment are needed for this measurement. At the time of writing, the new 20-foot target-calorimeter is being constructed in the muon area and is firmly on schedule.

In E319, the calorimeter is designed to provide a good measurement of  $v = E_o - E'$ . Especially at small value of  $\omega = \frac{2mv}{Q^2}$  and at large values of  $Q^2$ , measurement of  $E_h$  improves  $\frac{\Delta v}{v} \propto \frac{Q}{v}$  compared to when only spectrometer information ( $v = E_o - E'$ ) are used as shown in Figure 21. At the same time the target-calorimeter provides a direct measurement of hadron energy, thereby permitting a measurement of missing energy carried away by neutrinos in decays

$$X^+ \rightarrow \ell^+ + \nu + \text{hadrons}, \quad (7)$$

The improvements of our apparatus over E26 we are implementing are explicitly shown in Fig. 22.

These improvements are:

1. Better muon beam definition from using the beam chambers provided by E398.
2. "Wide angle muon catchers" will provide a large acceptance for decay muons which would escape from the spectrometer ( $\theta_{\mu}$  up to  $18^{\circ}$ ), thereby increasing the detection efficiency.
3. Fine-grained target calorimeter permits a hadron energy determination to 15%. (Figure 23)
4. New vertical trigger counter hodoscope installed in addition to the horizontal trigger counters used in E26. These counters form 25 "roads" for muons traversing the spectrometer. Pair triggers can easily be formed using the counter elements.
5. Rearrangement of trigger counter location. Trigger hodoscopes will be moved forward as closely as is possible. This arrangement will allow us to retain events which escape from the spectrometer before penetrating all spectrometer magnets.
6. All 8 toroid magnets will be turned on to optimize momentum resolution. For muons which traverse through all magnets, we can determine their momenta to  $\pm 10\%$  as compared to  $\sim \pm 14\%$  with only 5 magnets on in E26.



We shall describe our target calorimeter in some detail. Figure 22 shows a perspective view of the calorimeter. It consists of 120- 20" x 20" scintillation counters sandwiched between 1 7/8" target plate of iron, aluminum or CH<sub>2</sub>. 20 units of LECROY 2249A (12 channels each) will record the pulse height information. Both the normal gain or reduced gain ( $\times \frac{1}{10}$ ) output from the counter will be recorded thus permitting a faithful measurement of the energy of hadronic shower without saturation. The dynamic range of our calorimeter is about 250, with a charge sensitivity as low as 1 pico coulomb. The target plate size is 20" x 20", sufficient to contain all conceivable transverse spread of the shower as the incident muon beam is contained within  $\pm 4"$ . We already have all target plates on hand: 120 plates of Al, Fe and CH<sub>2</sub>. We plan to change target density during our run so that we can test experimentally whether or not our extra muons are "directly" produced without Monte-Carlo calculations. We believe that the target-changing feature cannot be duplicated easily by other similar muon experiments planned in the future.

#### V. Event Rate

Since we have already observed dimuons in our apparatus, it is quite easy to calculate the minimum number of multi-muon events from a  $10^{11}$  muon exposure.

For dimuons, the uncorrected rate is  $2 \times 10^{-3}$ /deep inelastic event. This is a lower limit since we have not corrected for detection efficiency and other losses.

Scaling this rate to this proposal we expect to observe a minimum of

$$32 \cdot \left( \frac{240}{72} \right) \cdot \left( \frac{10^{11}}{5 \times 10^9} \right) \cdot 2 = 3600 \text{ events.}$$

(Number of events observed in E26) (Ratio of target thickness) (Muon flux ratio) (Improvement in detection efficiency)

In reality we must change the target charge density periodically. This would reduce our total yields since the aluminum and  $\text{CH}_2$  target have less target density.

For the three sets of targets, we plan the following allocation of beam muons.

	Number of Muons	Minimum Number Of Dimuons
Fe	$6 \times 10^{10}$	2100
AL	$1.5 \times 10^{10}$	180
$\text{CH}_2$	$2.5 \times 10^{10}$	120
Total	$10^{11}$	2300

We note that the number of dimuons anticipated in our data exceeds the total dimuon yields expected from Experiment 310, the HWPF collaboration.

An event sample of this magnitude would permit a high statistic study of new particle production at high  $Q^2$ .

It may even "discover" the existence of a new hadron decaying leptonically especially when the missing energy is shown to be nonzero.

The missing energy  $E_M$  is defined by  $E_M = E_O - E_1 - E_2 - E_h$ . For a typical event where  $E_1 + E_2 + E_h = \frac{1}{2} E_O$ , the typical error on  $E_M$  is ~30%. The accuracy of  $E_M$  measurement improves rapidly as  $E_M$  increases.

#### VI. Running Time and Scenerio for this Exposure.

Our request is for an extension of  $10^{11}$  muon incident on our target-calorimeter during the coming muon running period. We have been approved 500 hours to perform a test of scaling in muon deep inelastic scattering. At the conclusion of E319 we are expected to pave the way for the next muon experiment E203/391. This latter experiment is scheduled to run in the next muon running period (>Spring, 1977). Our request does not delay appreciably this plan. We have further demonstrated that our target-calorimeter-toroidal magnet scheme works well for detection of multimMuon events and to permit missing energy measurements, a feature we did not have an opportunity to discuss earlier in the March, 1975 Muon Workshop at Fermilab due to insufficient time for analysis at that time.

We have all necessary hardware and software to record our data quickly. Since most of the new hadron searches have not yet proven conclusive, this proposed measurement

could well be a decisive one.

The energy calibration of our target calorimeter will be conducted in March, 1976. We plan to submit an addendum on the results of that calibration as well as further details on background estimates from accidentals, and other sources.

#### VII. NAL Contributions

No NAL contributions are needed.

#### References

1. Y. Watanabe et al, Physical Review Letters 35, 898 (1975)
2. C. Chang et al, Physical Review Letters 35, 901 (1975)
3. C. Rubbia, Talk at Palermo Conference, 1975

# E26 DIMUON EVENTS

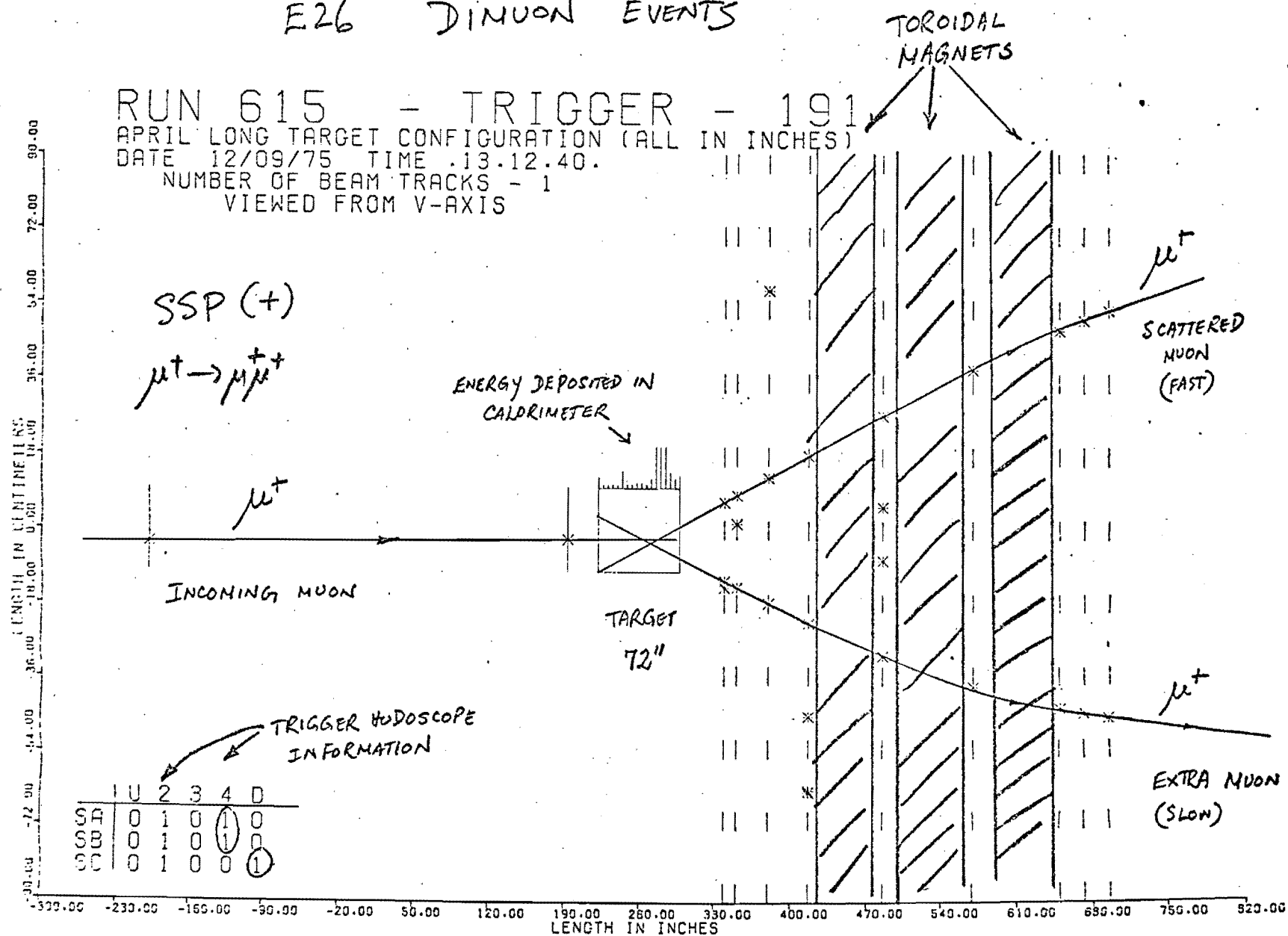


Fig. 1. TYPICAL DIMUON EVENT

RUN 617 - TRIGGER - 5776

APRIL LONG TARGET CONFIGURATION (ALL IN INCHES)

DATE 12/11/75 TIME 12.14.10.

NUMBER OF BEAM TRACKS = 1

VIED FROM U-AXIS

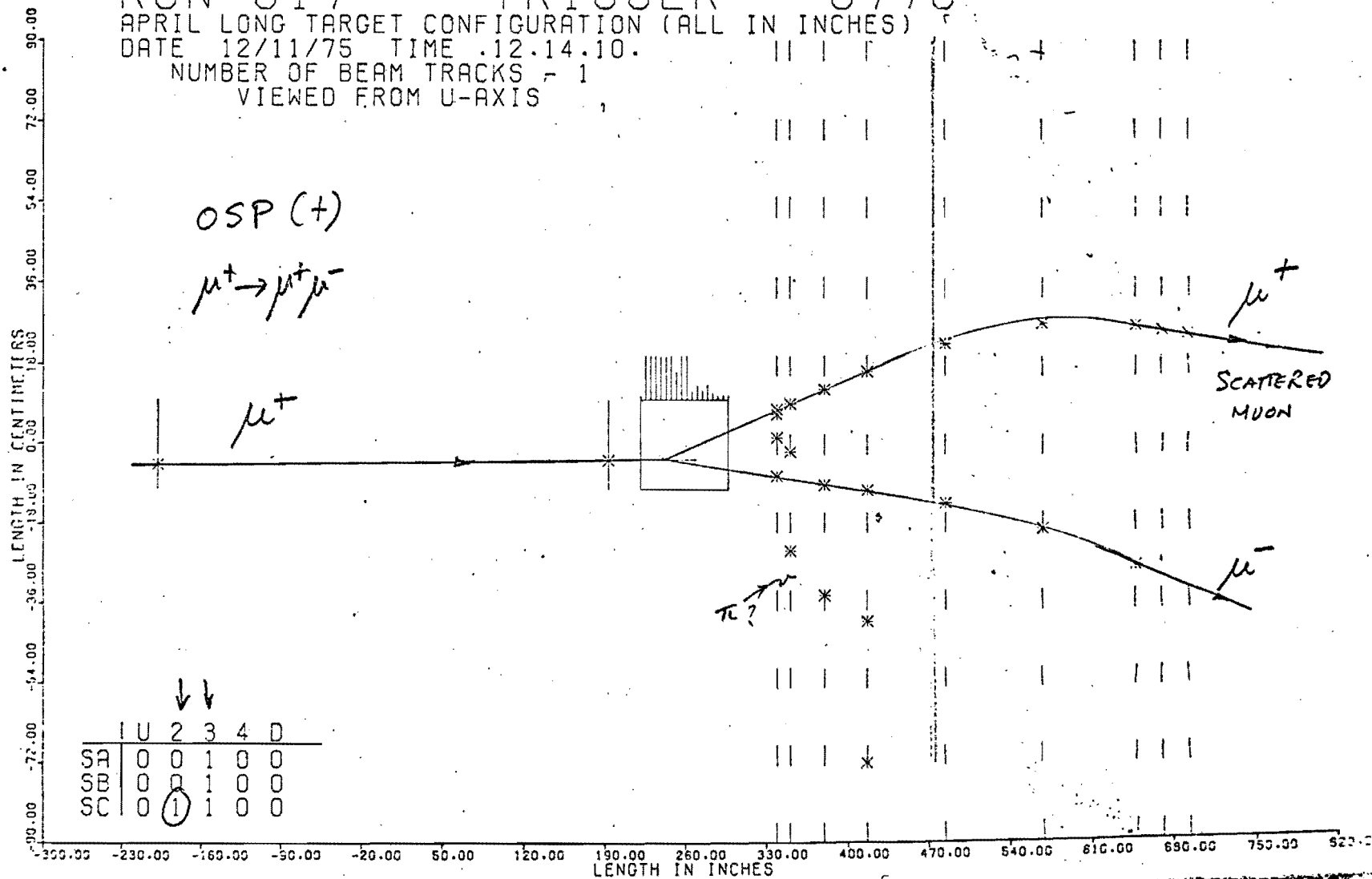


Fig.2 TYPICAL DIMUON EVENT

Fig. 3 TYPICAL DIMUON EVENT

SHOWS HALOS

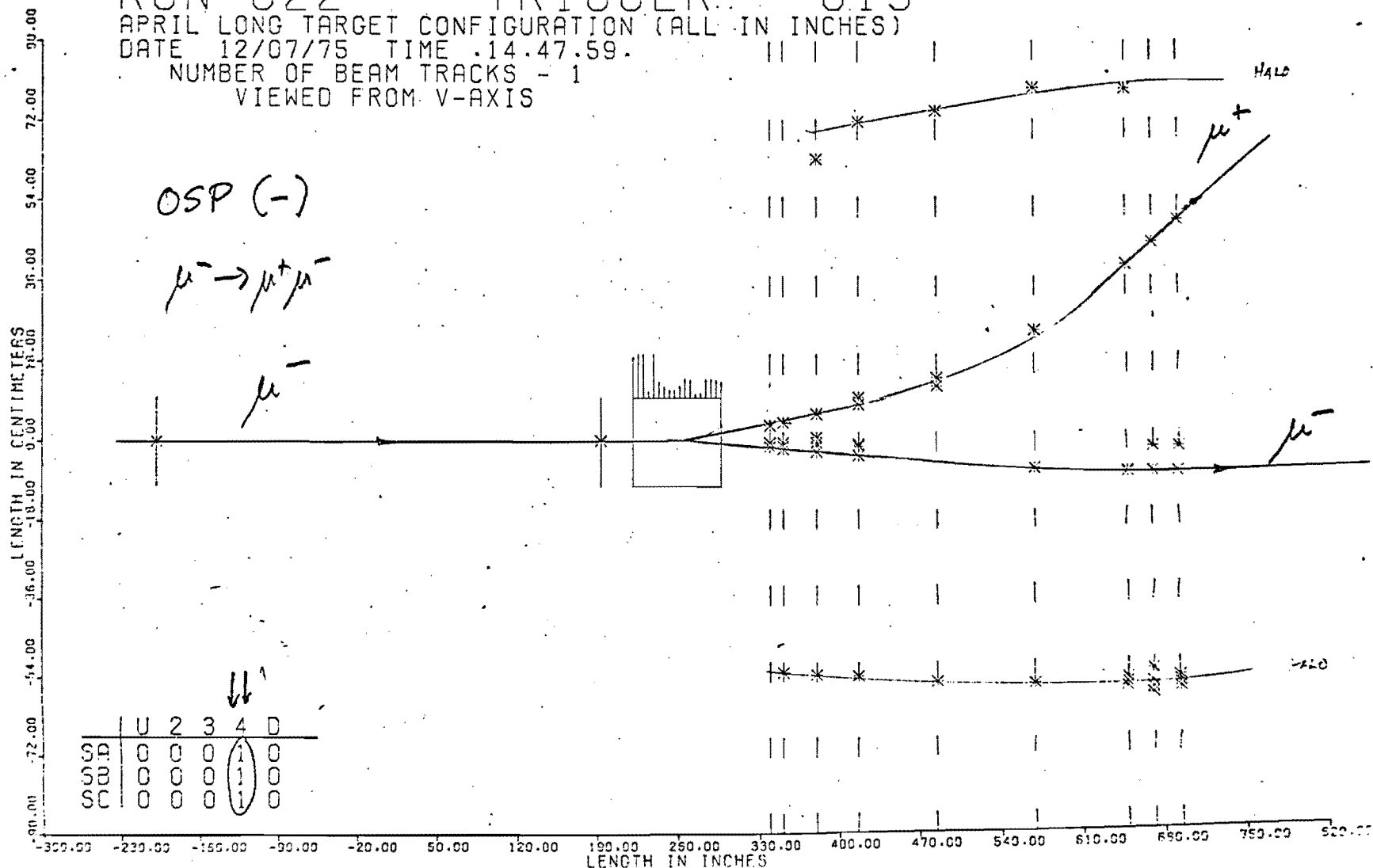
RUN 622 - TRIGGER - 813

APRIL LONG TARGET CONFIGURATION (ALL IN INCHES)

DATE 12/07/75 TIME 14.47.59.

NUMBER OF BEAM TRACKS - 1

VIED FROM V-AXIS



↓ ↓

	U	2	3	4	D
SD	0	0	0	1	0
SB	0	0	0	1	0
SC	0	0	0	1	0

Fig. 4 TYPICAL DIMUON EVENT

RUN 623 - TRIGGER - 2707

APRIL LONG TARGET CONFIGURATION (ALL IN INCHES)

DATE 12/08/75 TIME .11.50.02.

NUMBER OF BEAM TRACKS - 1

VIEWED FROM V-AXIS

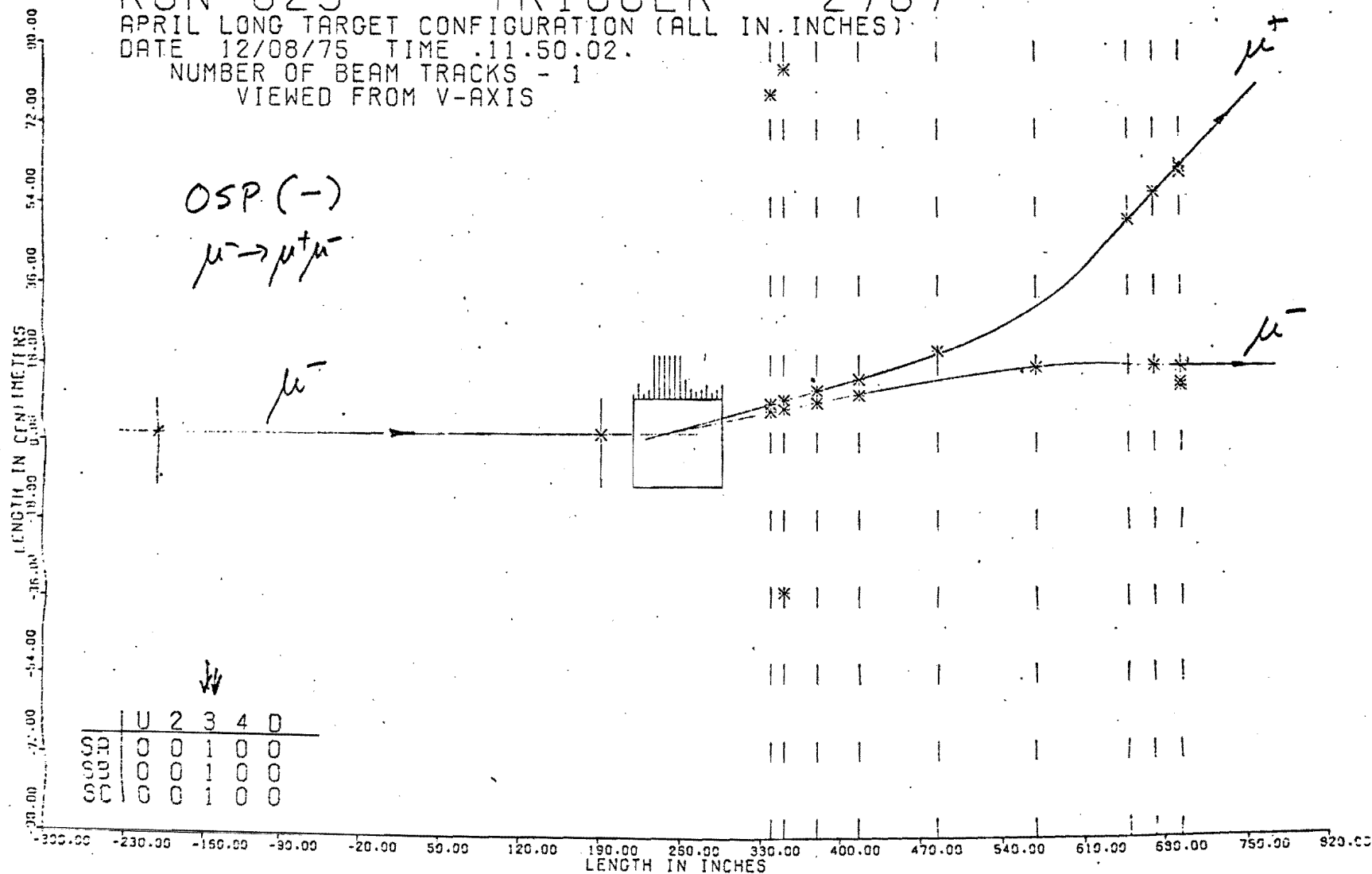




Fig. 5 TYPICAL DIMUON EVENT

RUN 626 - TRIGGER - 3691

APRIL LONG TARGET CONFIGURATION (ALL IN INCHES)

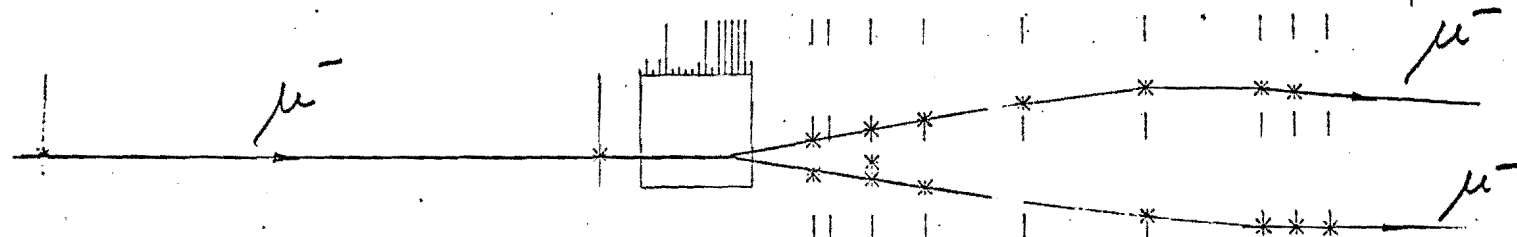
DATE 12/04/75 TIME 10.42.57.

NUMBER OF BEAM TRACKS - 1

VIED FROM X-AXIS

SSP(-)

$\mu^- \rightarrow \mu^- \mu^-$



↓ ↓

	1	0	2	3	4	0
SS	0	0	1	0	0	
SB	0	0	1	0	0	
SC	0	0	1	1	0	

100.00 130.00 160.00 190.00 220.00 250.00 280.00 310.00 340.00 370.00 400.00 430.00 460.00 490.00 520.00 550.00 580.00 610.00 640.00 670.00 700.00 730.00 760.00 790.00 820.00 850.00 880.00 910.00 940.00 970.00 1000.00

LENGTH IN INCHES

Fig. 6 TYPICAL DIMUON EVENT

RUN 630 - TRIGGER - 5496

APRIL LONG TARGET CONFIGURATION (ALL IN INCHES)

DATE 12/15/75 TIME .20.36.30.

NUMBER OF BEAM TRACKS - 1

VIEWS FROM X-AXIS

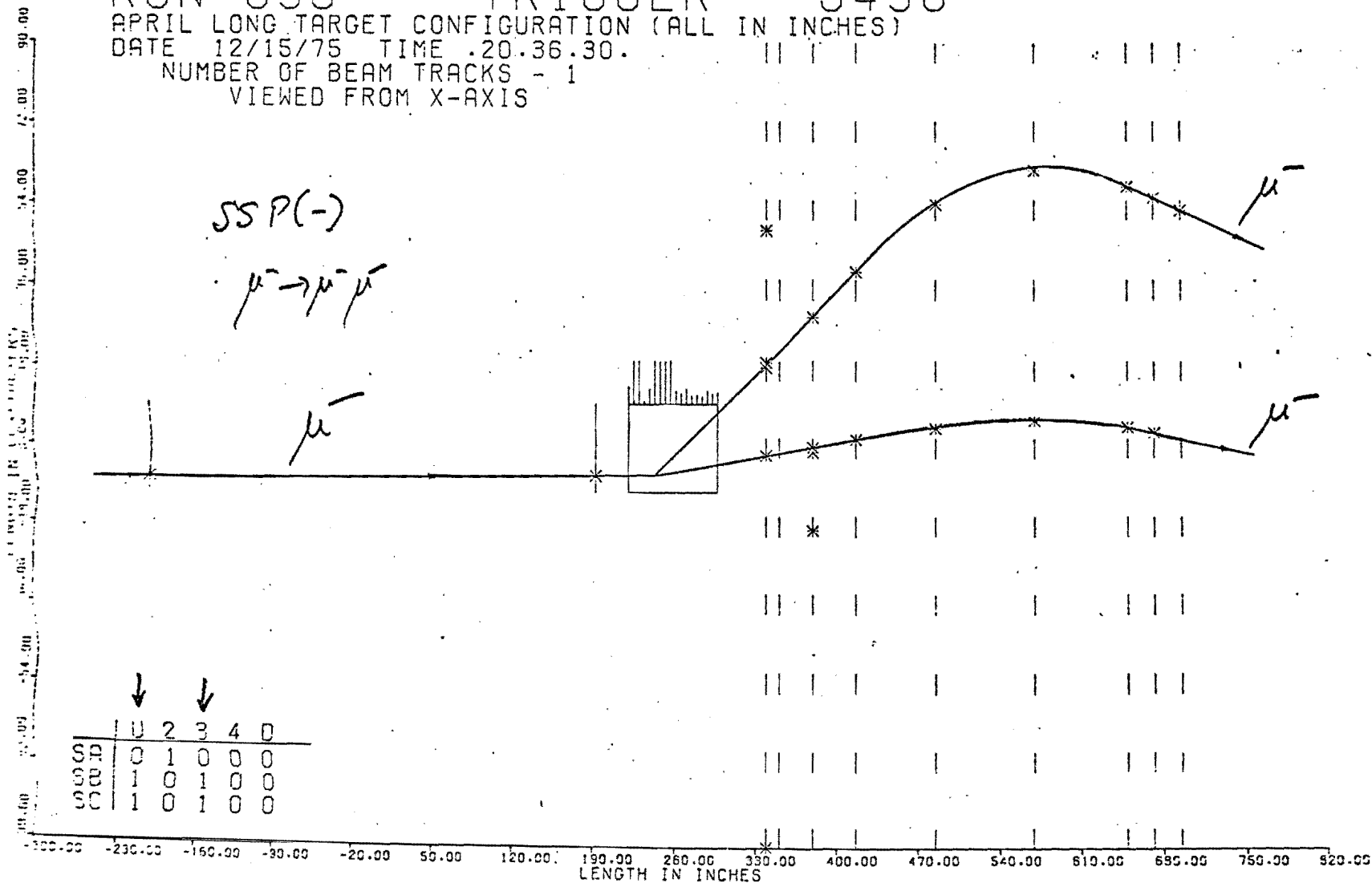


Fig. 7 TYPICAL DIMUON EVENT

RUN 632 - TRIGGER - 2814

APRIL LONG TARGET CONFIGURATION (FNAL-E26)

DATE 12/24/75 TIME .01.06.05.

NUMBER OF BEAM TRACKS - 1

VIEWED FROM U-AXIS

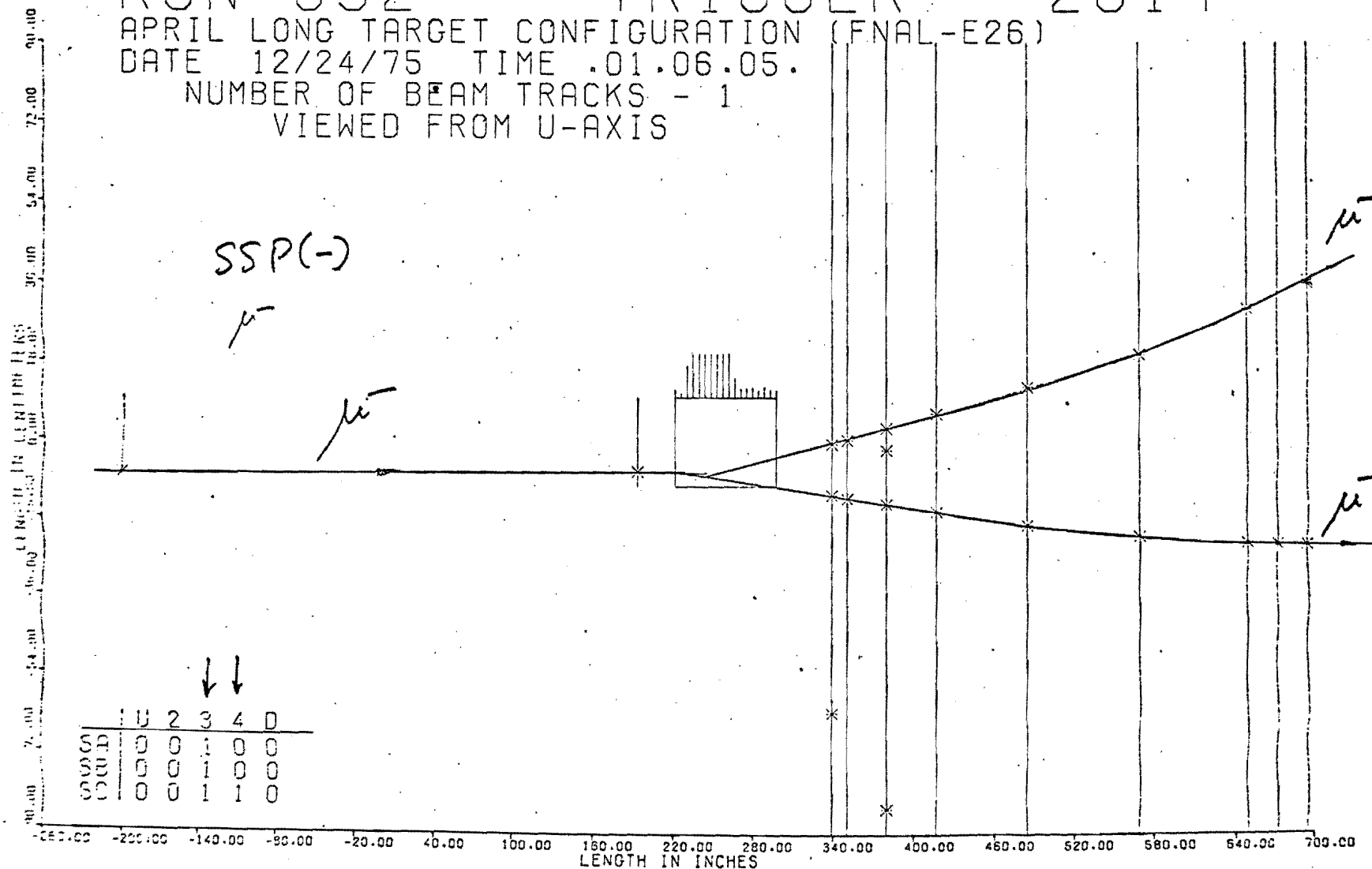


Fig. 8 TRIMUON EVENT

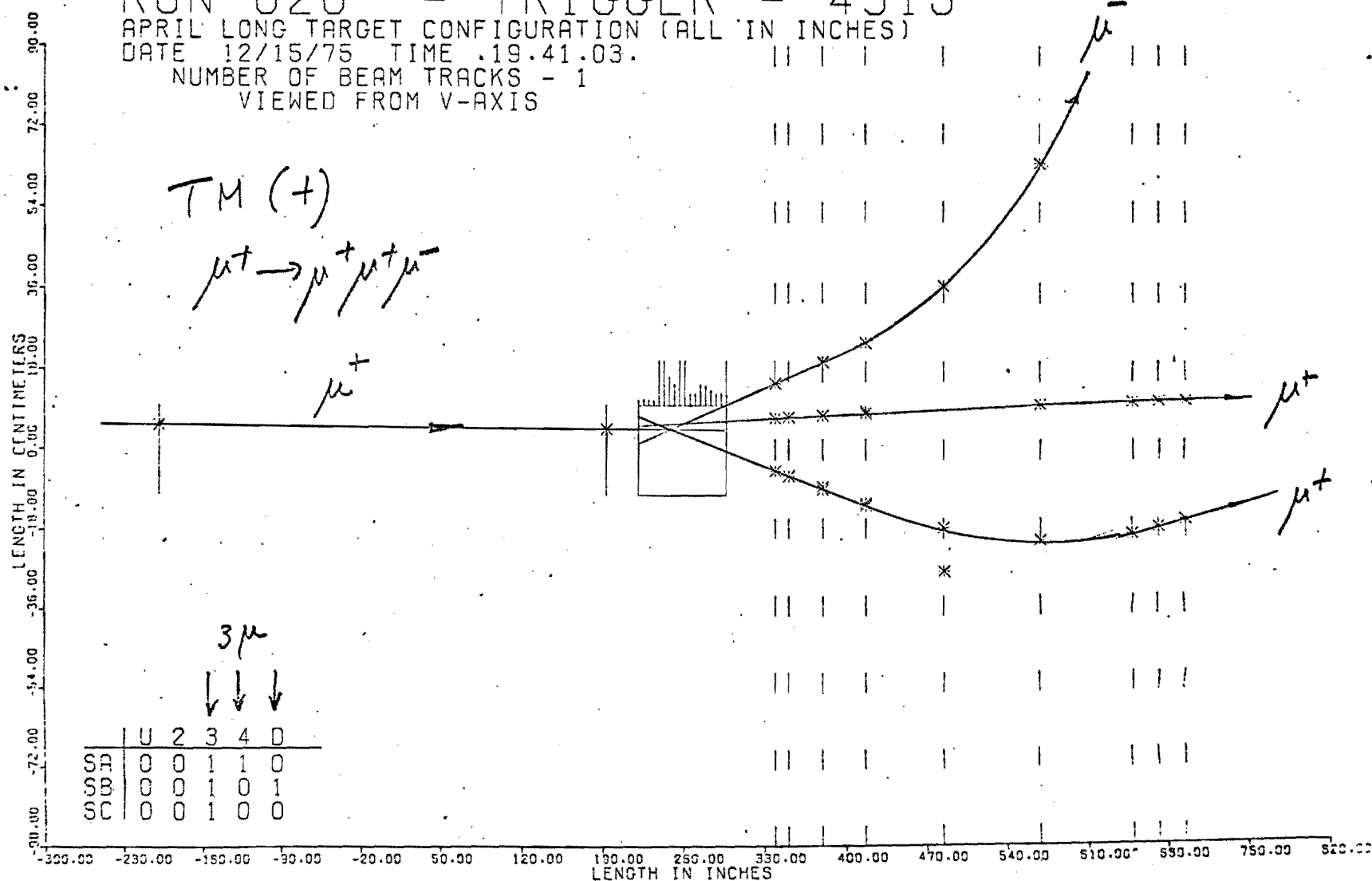
RUN 626 - TRIGGER - 4315

APRIL LONG TARGET CONFIGURATION (ALL IN INCHES)

DATE 12/15/75 TIME 19.41.03.

NUMBER OF BEAM TRACKS - 1

VIEWED FROM V-AXIS



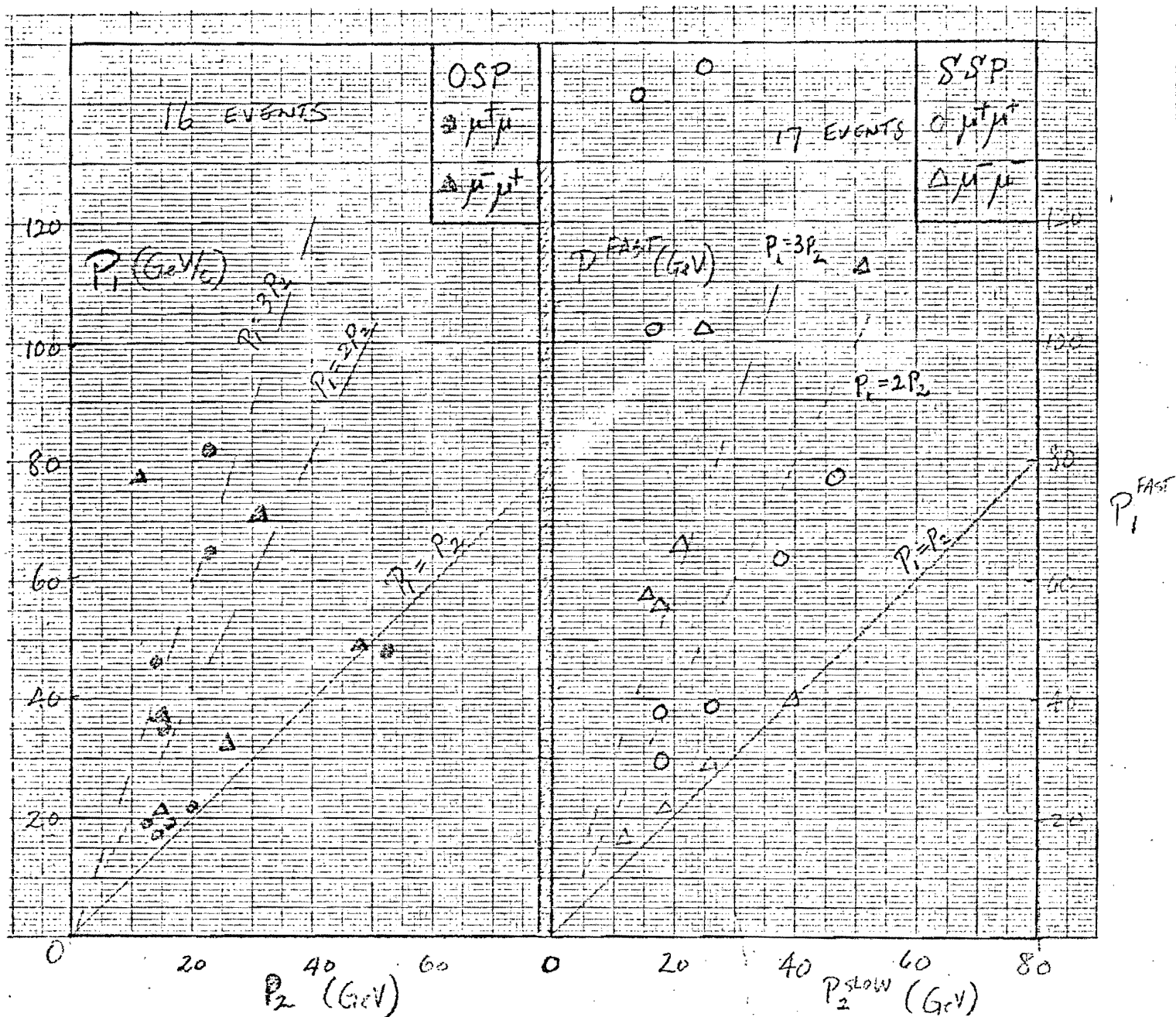


Fig. 9 Momentum of the leading muon versus the momentum of opposite sign muon for OSP events. The lines are for  $P_1 = P_2$ ,  $P_1 = 2P_2$ ,  $P_1 = 3P_2$ . Note the leading-particle effect ( $P_1 > P_2$ ).

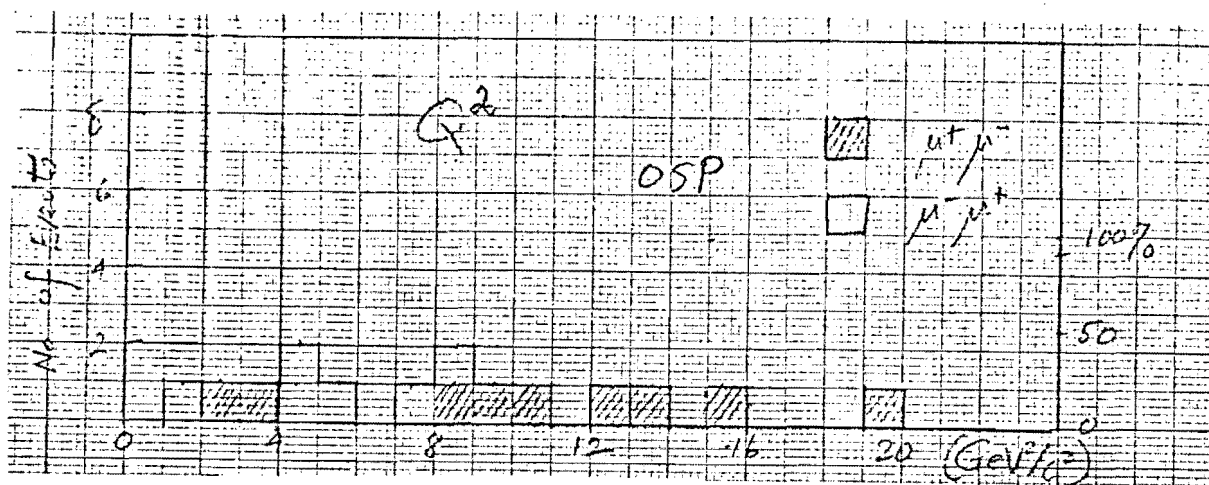


Fig.10  $Q^2$  distribution for OSP pairs

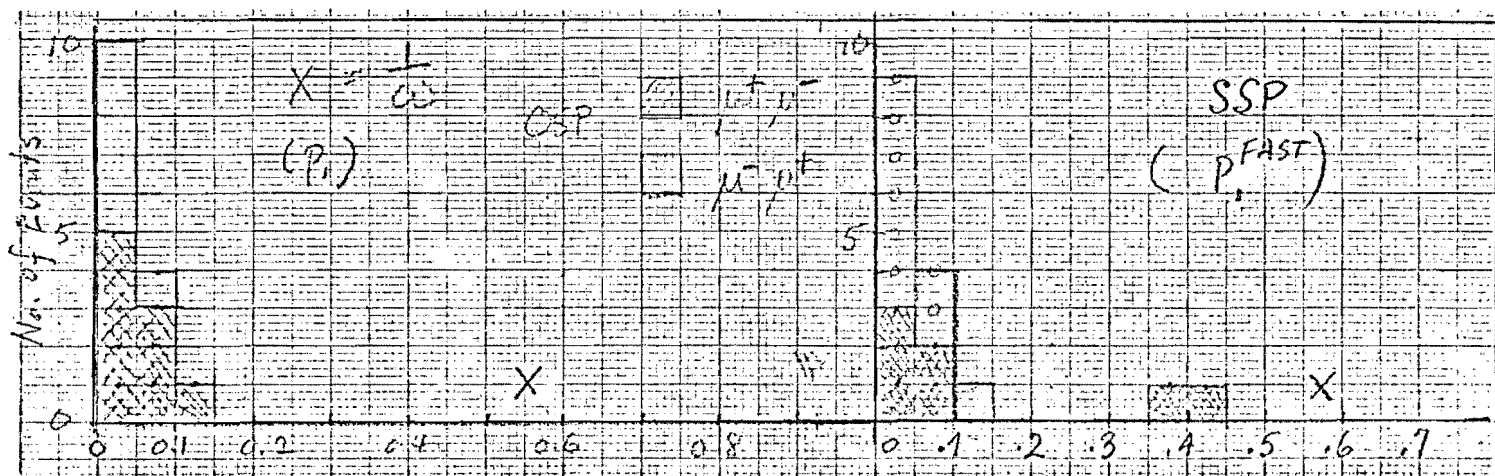


Fig.11  $x$  distribution for OSP pairs

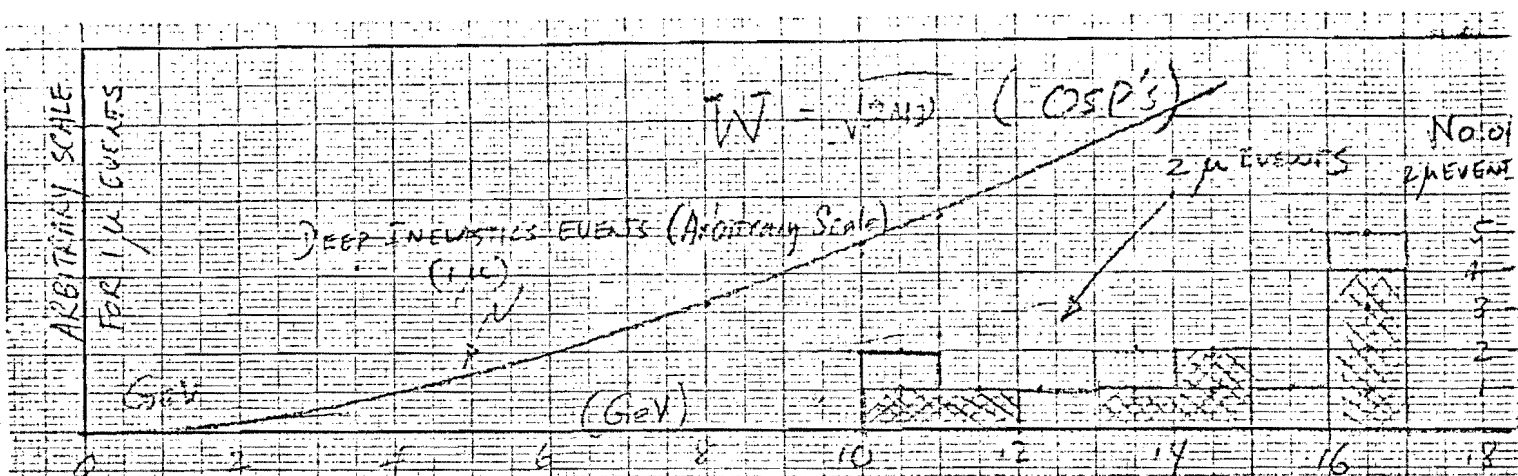


Fig. 12 Missing mass distribution for  $\gamma_v$ -N system.  
The scale for single muon events is arbitrary

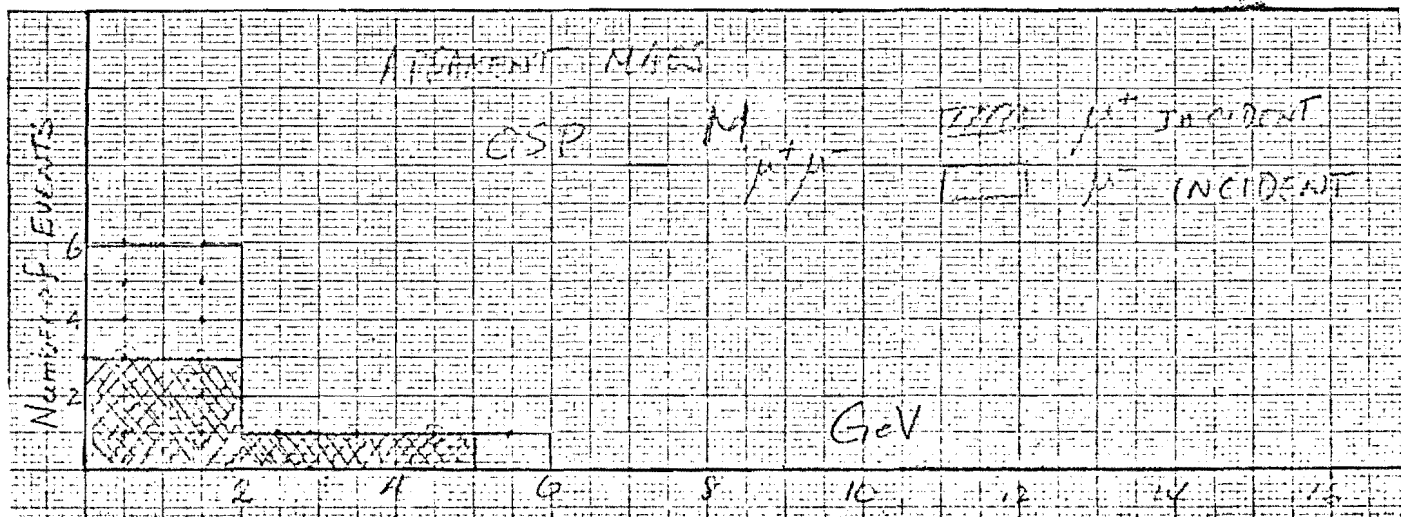


Fig. 13 Apparent mass distribution between pairs for OSP's

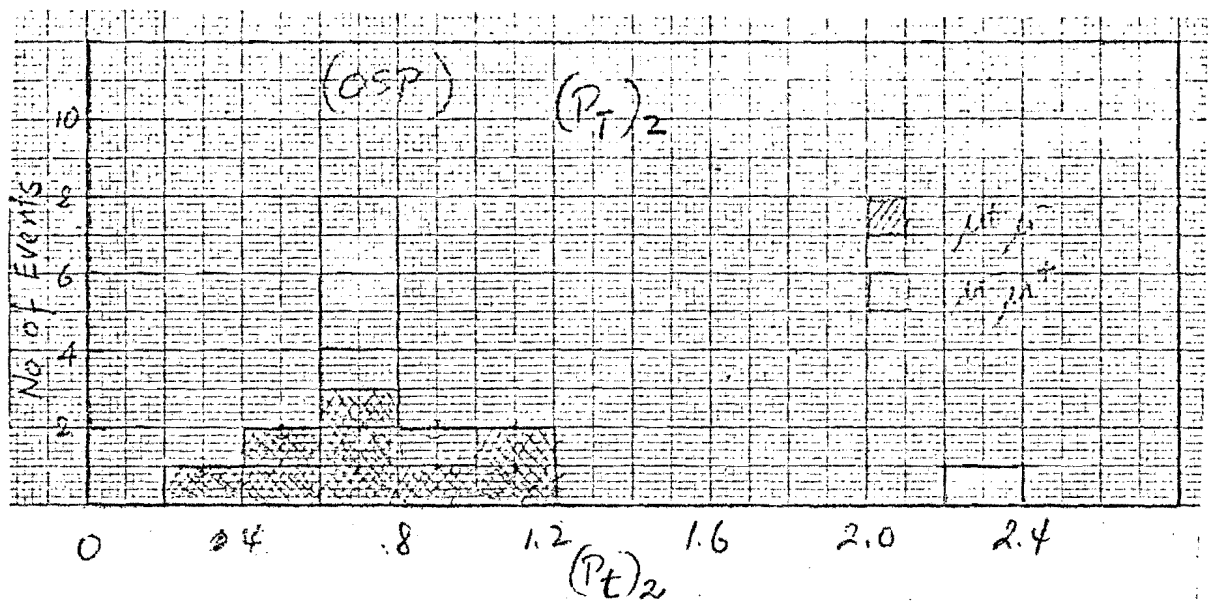


Fig. 14 Transverse Momentum distribution with respect to the virtual photon direction for OSP pairs

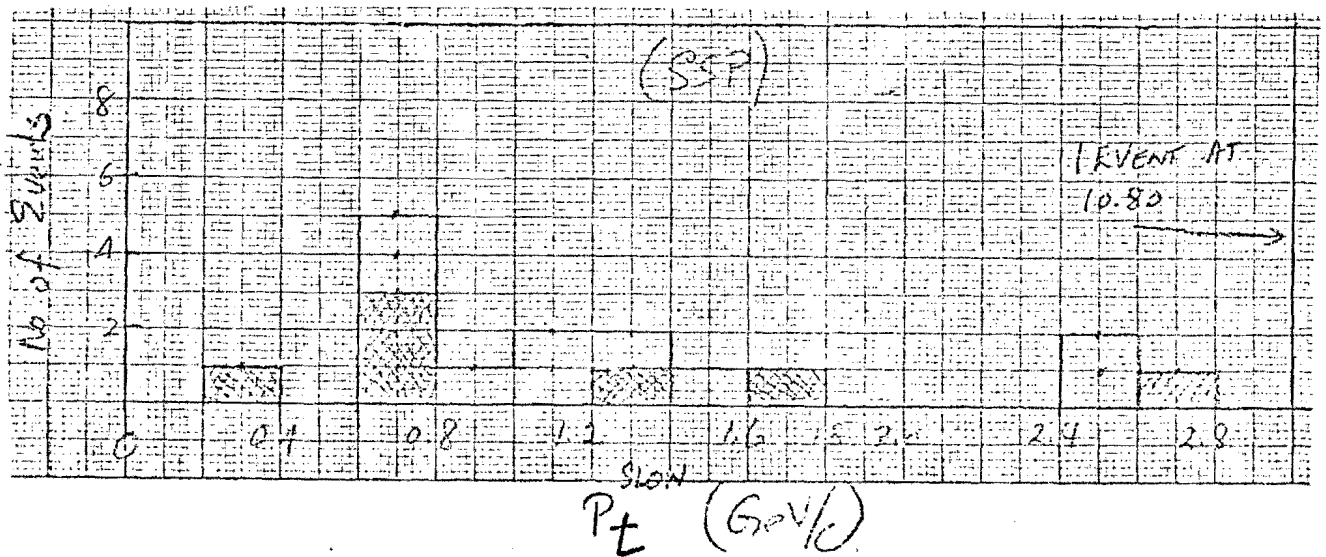


Fig. 15 Transverse momentum distribution with respect to virtual photon distribution for SSP pairs.  $P_{1\text{FAST}}$  was used to define  $\gamma_v$  direction



# EIA DATA (2 DIMUONS)

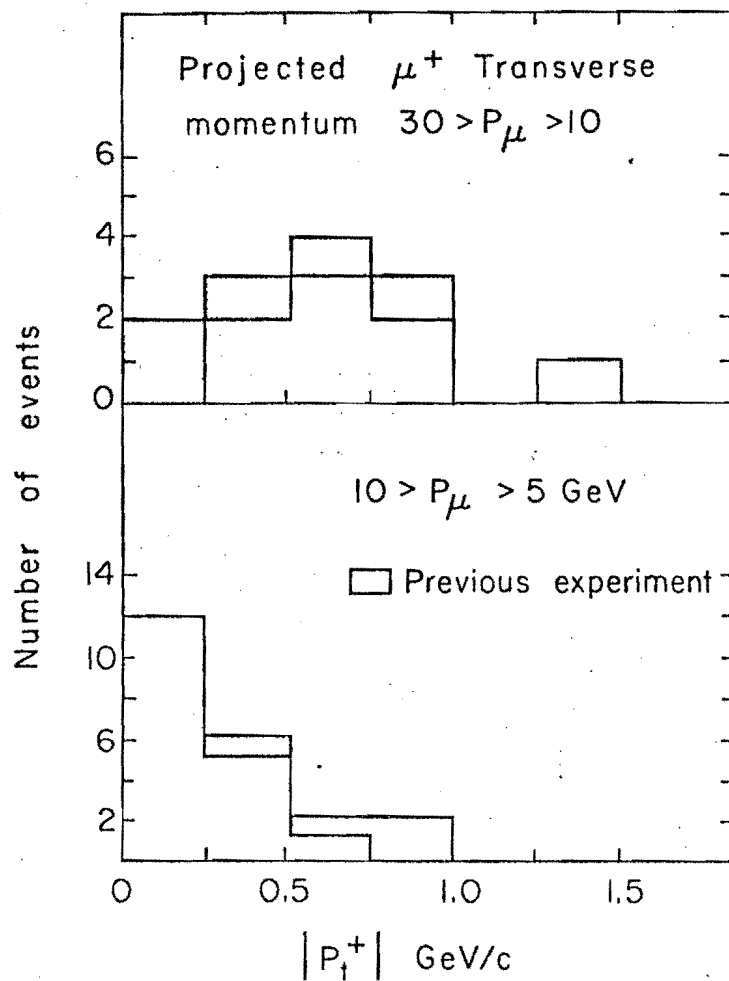


Fig. 16 Transverse momentum distribution with respect to the  $\mu^-$ - $\nu$  plane for all  $\mu^+$  momenta

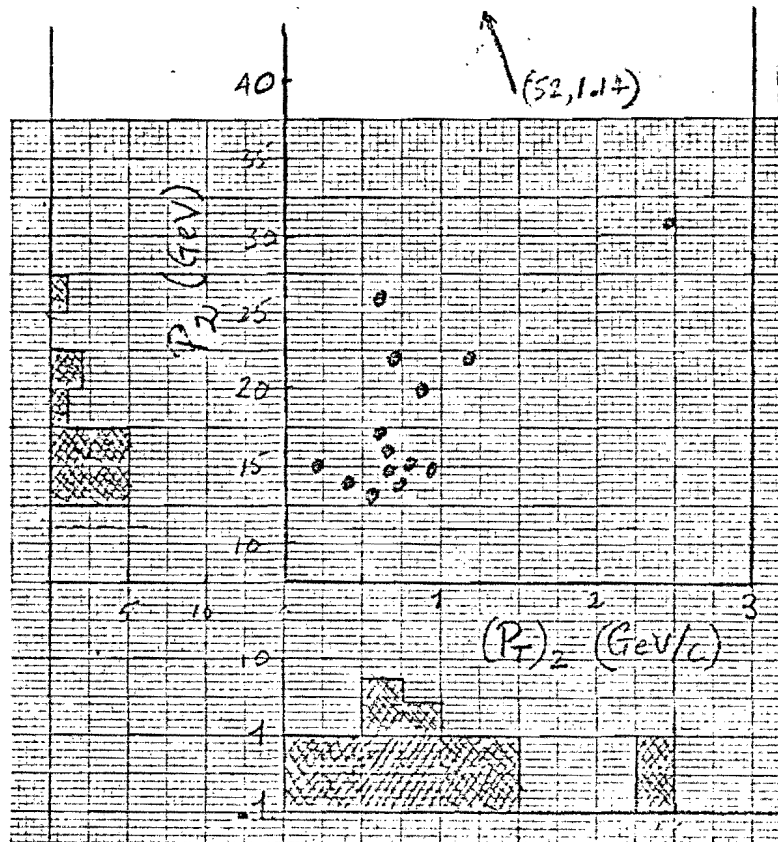


Fig. 17 Momentum of "extra muon" vs  $P_t$  for opposite sign pairs

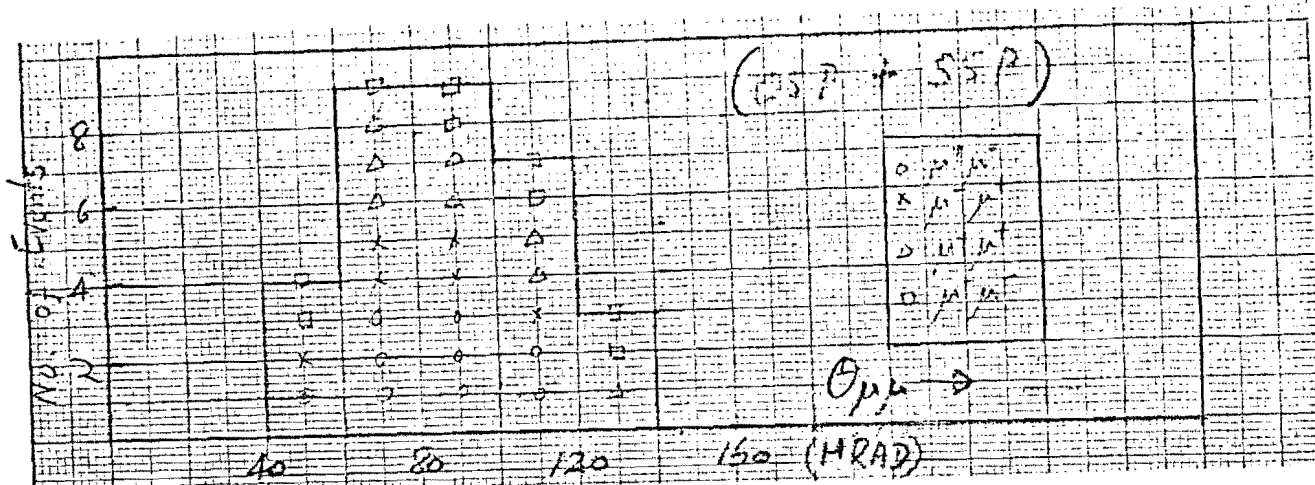


Fig. 18 Opening angle distribution for all pairs (OSP + SSP). 32 Events

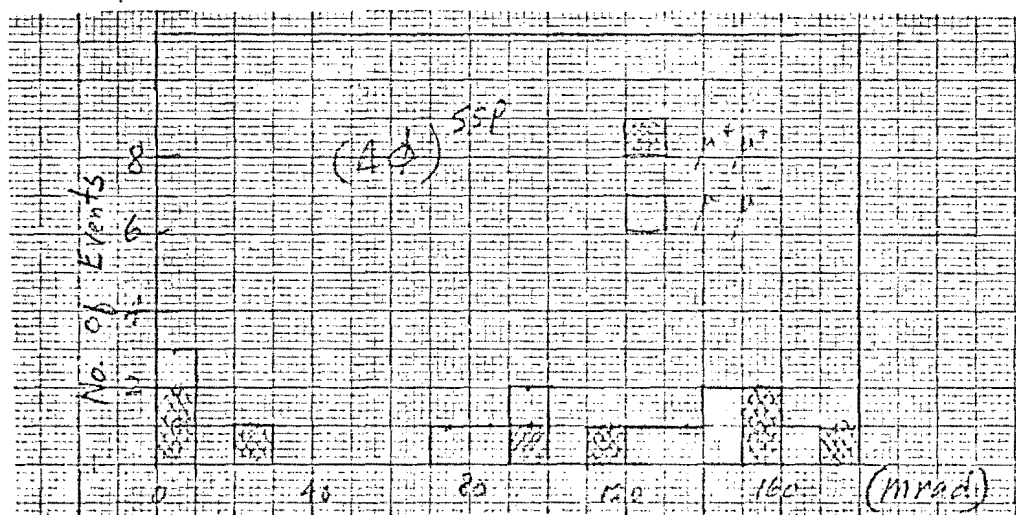
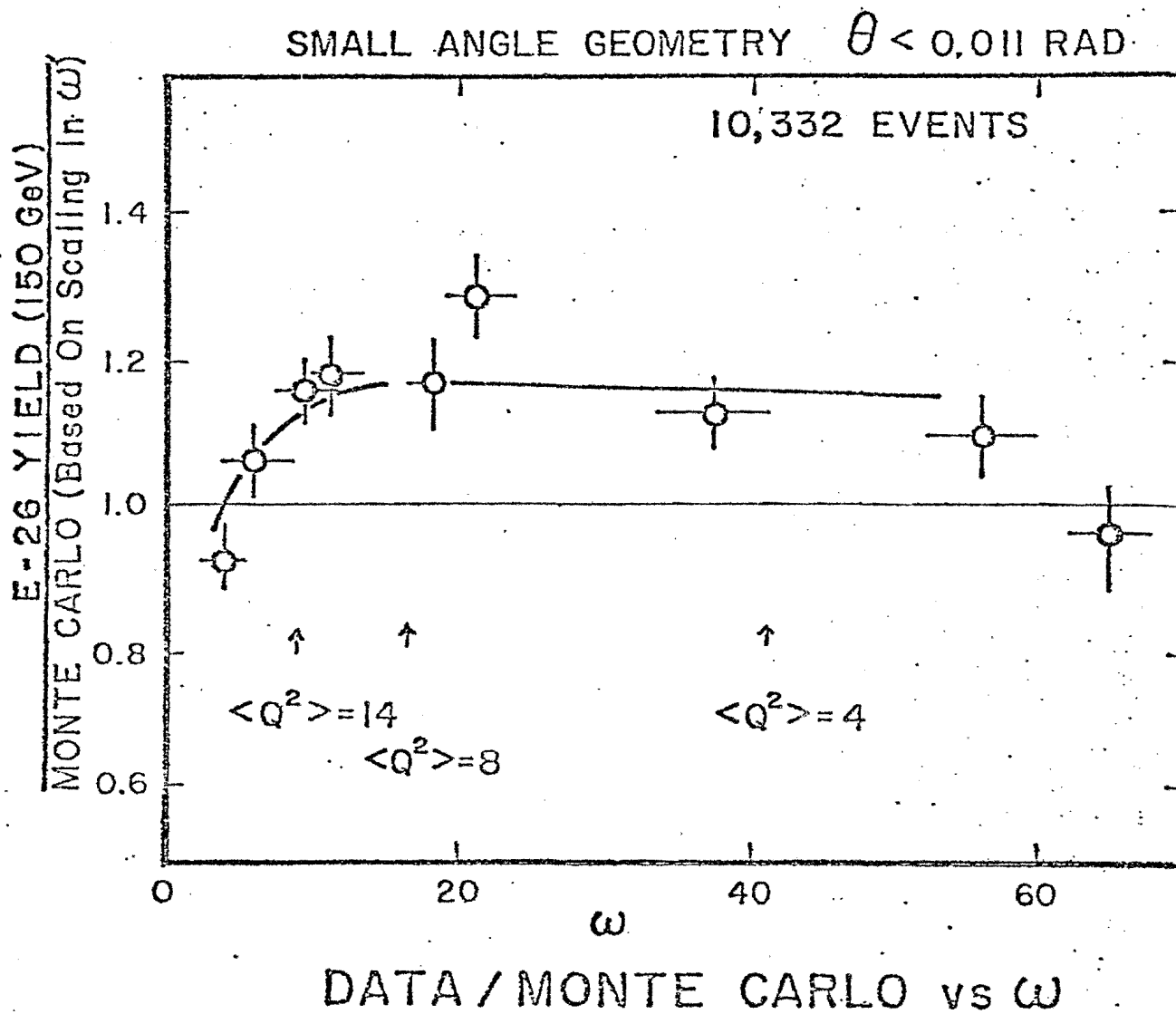


Fig. 19 Azimuthal angle between muons for all pairs (OSP + SSP). 32 Events



20  
Figure 20

# $\nu$ RESOLUTION AT ENERGIES IN P 319

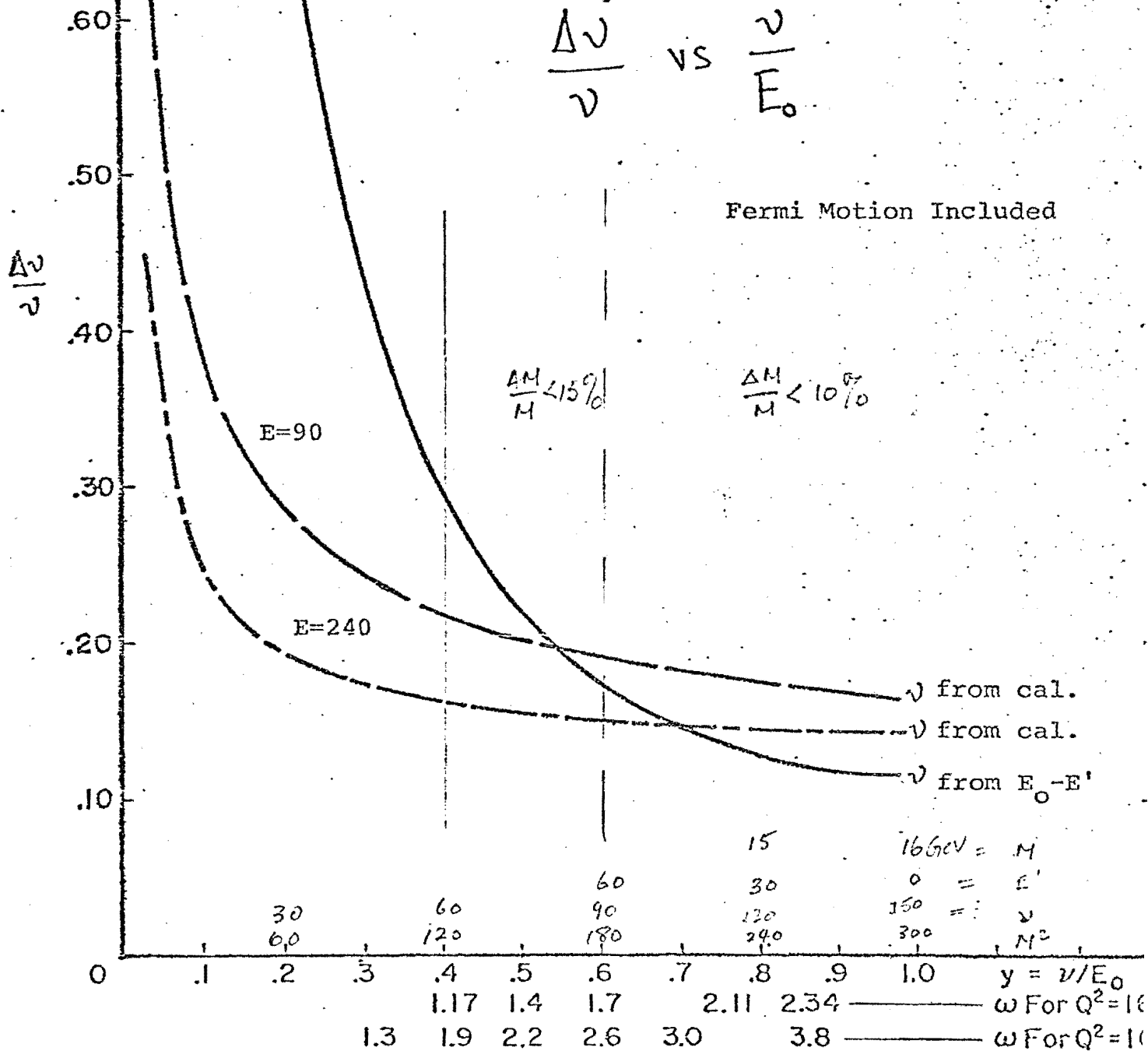
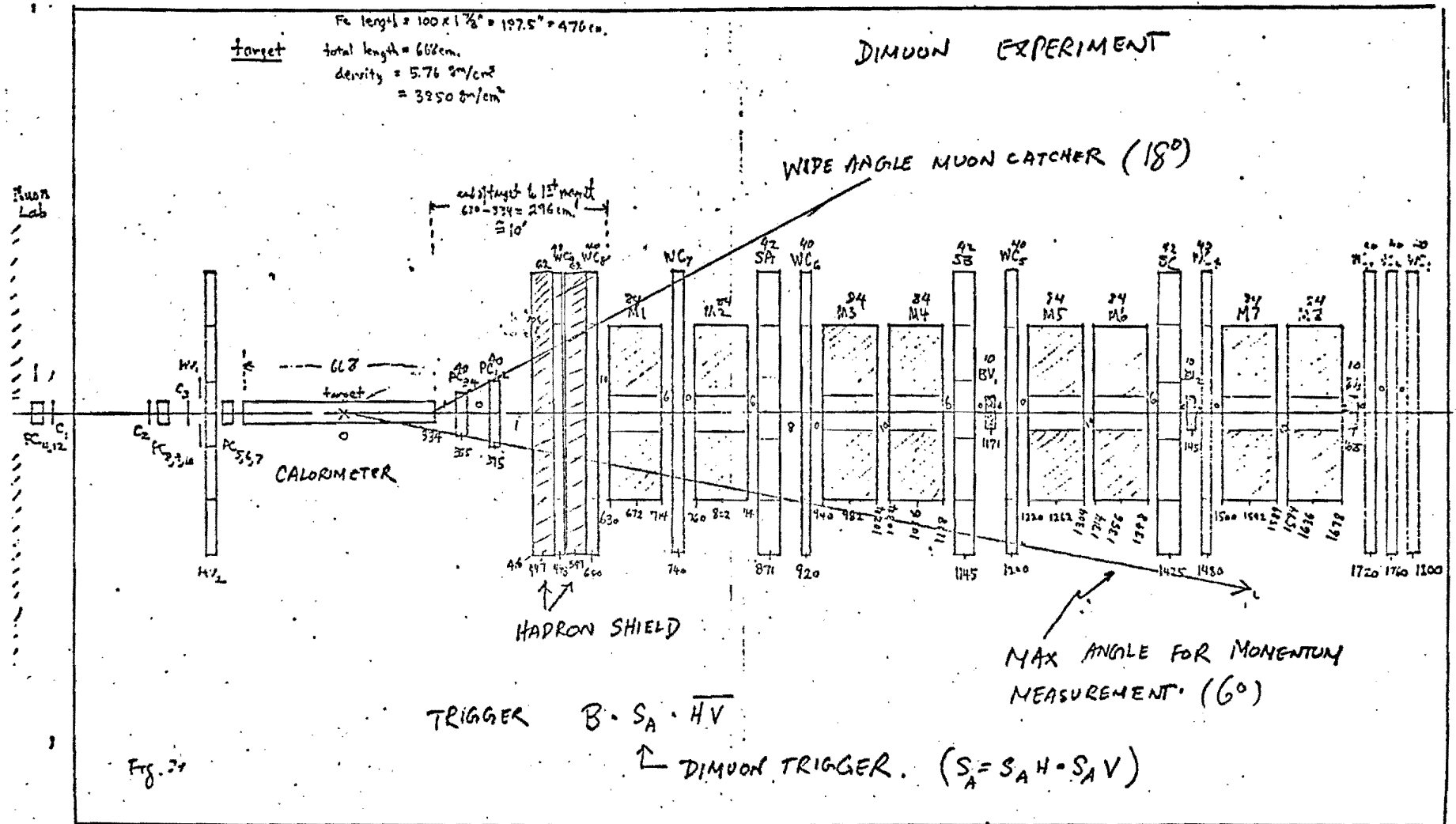
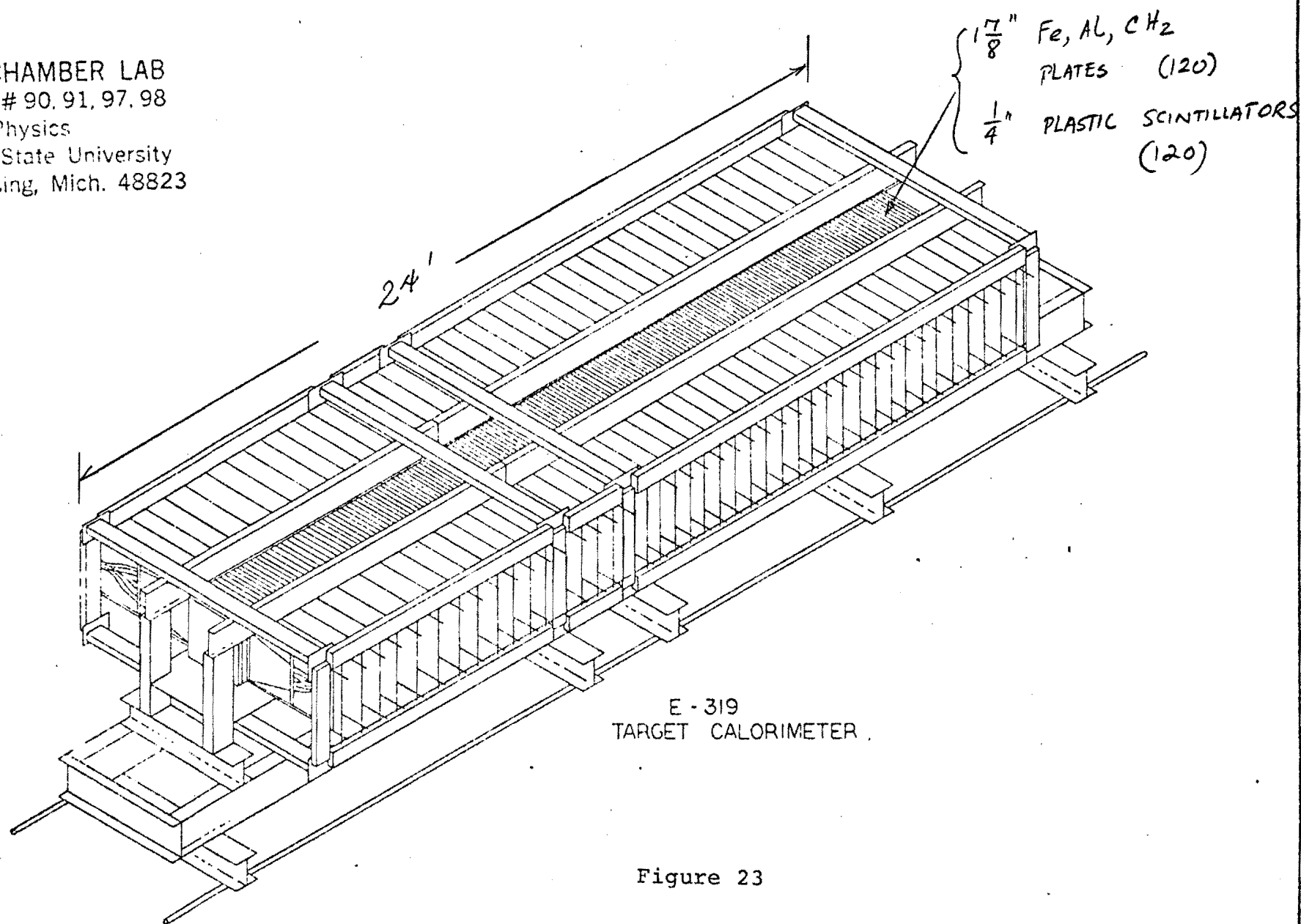


Fig 21 Figure 21



SPARK CHAMBER LAB  
Quonsets # 90, 91, 97, 98  
Dept. of Physics  
Michigan State University  
East Lansing, Mich. 48823



ADDENDUM TO PROPOSAL 474

A Detailed Study of "Extra Muon" Production in Deep Inelastic  
Muon Interactions

E-319 Group

March 1, 1976



# INTRODUCTION

Following the proposal presentation meeting on February 5, 1975, we have been asked to present further documentation on a few questions not thoroughly discussed earlier. This addendum attempts to answer some of these questions.

We now believe a run of 500 hours at 300 GeV or  $7.5 \times 10^{10}$  muons can satisfy all requirements for P-474.



Fermilab

Fermi National Accelerator Laboratory  
P.O. Box 500 • Batavia, Illinois • 60510

Directors Office

February 11, 1976

Ref: #474

Professor K. Wendell Chen  
Physics Department  
Michigan State University  
East Lansing, Michigan 48823

Dear Wendell:

I am writing to acknowledge formally our receipt of your recent proposal entitled "A Detailed Study of "Extra Muon" Production in Deep Inelastic Muon Interactions". I have assigned the designation P-474 to this proposal and it has been distributed to our Program Advisory Committee. I would also like to thank you for coming to our meeting last Thursday to give an oral presentation of this proposal.

In the discussion that followed last Thursday's meeting it was agreed that it would be useful to have some additional documentation from you prior to the Program Advisory Committee meeting in March. To be specific, we find very significant the question of whether or not it would be possible to run E-319 and P-474 simultaneously within the existing approval for E-319. We felt that you had not fully considered this possibility prior to last Thursday's meeting and we would now appreciate a further response from you regarding the implications this would have for both experiments. I think it is fair to say that those of us that participated in the discussion following the meeting were still unclear at that point on the triggering scheme you had in mind for P-474 and how it differed from that for E-319.

There were also some questions raised regarding how you would handle systematic effects in your dimuon data sample. The possible confusion caused by tridents was noted in particular in instances where one of the trident tracks passes through the hole in your toroid magnets or, alternatively, where one of the trident muons stops in the target. I think we would welcome any further comments you feel you can make about your ability to handle the systematic effects you would be likely to encounter in P-474.

I hope you will be able to respond to the above in the very near future. However, if at all possible please see that we receive your response by Monday, March 1. This will enable

us to have the material available to the PAC members who arrive at the Laboratory a day or two early to complete their preparations for the meeting.

Thanks for your help.

Sincerely yours,

*Tom*

T. H. Groves

# I. Can our Dimuons be Tridents in Origin?

We examined in some details the kinematical properties of QED tridents.

If one of the muons in a QED trident should have an energy less than a few GeV, the event may fake a dimuon event when the low energy muon stops in the target. Tridents with muons emitted in the forward direction will be vetoed if  $\theta_{\mu} < \theta_{\text{cut}}$  defined by the beam veto counter.

In order to study these effects, Monte Carlo trident events were generated according to the Bethe-Heitler trident cross section defined by Brodsky and Ting (Phys. Rev. 145, 1018 (1966), for 150 GeV muons on an iron target. The elastic form factor for an iron nucleus was taken as

$$\exp \left( -\frac{b^2}{6} Q^2 \right) / \left( 1 + \frac{c^2}{6} Q^2 \right),$$

where  $b = 24 \text{ fm}$ .  $c = 1.07 \times A^{1/3} \text{ fm}$ . Events with a muon of  $E > 5 \text{ GeV}$  and  $\theta_{\mu} < \theta_{\text{cut}}$  were rejected. Muons with  $E < 10 \text{ GeV}$  were considered undetected. The probability that this could happen as a function of  $\theta_{\text{cut}}$  is shown in the following table.

$\theta_{\text{cut}}$ (mr)	Probability (%) ( $\pm 3\%$ )
1	6.2
2	7.7
3	3.6
4	3.4

Our studies show that only up to 7% of all tridents will have a low energy muon stoppable by the target or by other parts of the apparatus. The remaining 93% of tridents are detected with reasonable efficiency. This endorses

our belief that the dimuon sample cannot all be of QED in origin unless the ratio of detection efficiencies for tridents is only 1.4% of that for dimuons. This is highly unlikely as we believe the efficiencies for muon detection is of the order 50%.

- B. A possibility exists that the third muon of the trident events may enter the "dead" region in the center of muon spectrometer. However, since beam veto was included in our trigger, events of this kind would have been vetoed with high efficiency.

Dimuon event losses caused by the beam veto counter can be crudely estimated by examining the opening angle distribution of the observed dimuons. As is shown in Figure 18 of the original proposal,  $\langle \theta_{\mu\mu} \rangle$  is  $\sim 85$  mrad. Since the angle subtended by the hole and the veto counter is always less than 17 mrad, we estimated a loss of 30% or less, due to finite size of the muon beam.

## II. Can P-474 be run with E-319?

A. A question has been raised regarding whether it is possible to run E-319 (Bjorken scaling tests) and P-474 (Dimuon studies) simultaneously within the existing approval for E-319.

To answer this question we first discuss plans for E-319 with respect to our allocation of beam muons to each of the four required runs. (See Appendix I). We feel that the E-319 runs cannot fully accommodate our objectives in P-474 under optimum conditions. We present our reasons below:

1. Total muon flux available in E-319 at  $E_{\mu} = 300$  GeV is inadequate.

We note that in the existing approval of 500 hours for E-319 (we requested  $3 \times 10^{11}$  muons) we can only expect an integrated flux of  $7.5 \times 10^{10}$  muons, (including low energy muon runs) This is due to the fact that the repetition rate for NAL is now only 1/2 (400 GeV) of that anticipated earlier.

As is discussed in Appendix I, we plan to run only 250 hours at  $E_{\mu} = 300$  GeV. Thus the muon flux useful for dimuon work ( $E_{\mu} = 300$  GeV) would be less than  $2.5 \times 10^{10}$  or 1/4 of the total requested in P-474.

2. Dead-time losses due to single deep inelastic muon triggers could be troublesome. Our maximum data-taking rate is limited to 30 single muon triggers/pulse. Attempts will be made to reduce our trigger rate to maximum allowable to prevent ~~dead~~-time loss to dimuon rates. If this is not possible, muon triggers "OR"ed with single  $\mu$  triggers will suffer corresponding dead-time losses.
3. E-319 would not have adequate time to study yields at different target density.

40% of running time requested in P-474 will be devoted to running with Al and CH<sub>2</sub> targets. (originally we anticipated to study A dependence with these targets). At this moment, no beam time is allocated for runs with targets other than iron in E-319.

It would seem to us that even with the most optimum E-319 scenerio that all dimuon triggers are "OR"ed with single  $\mu$  triggers successfully without dead-time losses, we will still collect only 1/4 of data expected in P-474. There will be no data taken using different density targets. This would be serious since one would have to depend on Monte-Carlo calculations to estimate the  $\pi, K$  decay backgrounds.

We thus conclude that an extension of 500-750 hours should be satisfactory to run P-474:

1. We can run exclusively with dimuon triggers, high  $P_T$  triggers or large energy loss  $\mu$  triggers, thus maximizing dimuon rate.
2. Collect data to obtain dimuon yields at infinite target density.
3. We benefit from having a set of hodoscopes at the "wide-angle muon catcher." This set of hodoscopes is not planned in E-319.  
Systematic corrections could be better understood.
4. We can make use of our last trigger bank  $S_C$  to select  $P_T$  continuously to determine precisely optimum triggers to minimize backgrounds.  
This can only be achieved by moving  $S_C$  from inside the spectrometer to the rear of spectrometer. [Figure 1 and 2]

#### B. Possible Trigger Arrangements for P-474

We have been considering triggers that are more efficient in picking out multimuon events and yet that could possibly be operated in parallel with

the single muon trigger used in E-319. One possible trigger is described below. We shall not discuss high PT triggers or large energy loss triggers.

Three sets of hodoscopes,  $S_A$ ,  $S_B$ , and  $S_C$ , are used to define the scattered muon in E-319. For P-474, we plan to use only the first and second set, located behind the second toroid and 3-ft. hadron shields. The arrangement of these counters are shown in Figure 1.

$S_A$ ,  $S_B$  each consist of two hodoscopes:

$S_{AH}$ ,  $S_{BH}$  = horizontal counters, 5 each 14" wide

$S_{AV}$ ,  $S_{BV}$  = vertical counters, 5 each 14" wide

These hodoscopes define 5 x 5 non-overlapping regions adjacent to the magnetized toroids. The dimuon triggers can be formed by requiring the simultaneous presence of two penetrating particles in coincidence with the muon beam. Thus, we symbolically define a trigger as follows:

$$\text{Dimuon Trigger} = B \left\{ \sum_{j=1}^5 \sum_{\ell=1}^5 (S_{AH}^i \cdot S_{AV}^j) \cdot (S_{BH}^k \cdot S_{BV}^\ell) \right\} \cdot \overline{HV}$$

$i=1 \quad k=1$

or abbreviated as  $B \cdot S_A \cdot S_B \cdot \overline{HV}$ .

where B is the beam, HV is the halo veto. (See Fig. 22 on original proposal).

The minimum angle for muons is determined by the inner size of the toroids with a 12" diameter hole. If necessary, by choosing suitable additional correlations of coincidences between  $S_A$ ,  $S_B$ , and  $S_C$ , the trigger can be limited further to those crossing a region about the target in both horizontal and vertical directions. This feature may be necessary to reject high trigger rates caused by halo beam muons in the same RF bucket with beam muons, or electromagnetic and hadronic showers.



B. We have not yet decided on the trigger scheme for dimuon experiment.

If we adopt the high  $P_T$  single muon trigger, the placement of  $S_C$ , (third trigger hodoscope) might have to be moved to the rear of our spectrometer so that the value of  $P_T$  can be varied up to over 2.0 GeV/c. During the experimental tune-up, the trigger rate studies will be done.

The dimuon event rate is estimated to be  $\geq (2 \times 10^{-3}) \times (2.6 \times 10^{-5}) = 5.2 \times 10^{-8} / \text{muon}$ .

This rate is considerably smaller than the expected background trigger rates listed below in order of their expected magnitude:

- 1) Single  $\mu$  scattering giving  $\nu > 25$  GeV. The associated hadronic shower penetrates 12-ft. of iron (4 toroids and 3-ft. of hadron shield). This probability of penetration is  $10^{-4}$ . Combined trigger rate is  $(6.5 \times 10^{-3}) \times (10^{-4}) \approx 6.5 \times 10^{-7} / \text{muon}$
- 2) Inefficiency in vetoing RF buckets in which we have both a halo and a beam muon. The beam muon interacts and scatters with  $\nu > 15$  GeV. The combined probability is  $(0.02) \times (10^{-3}) \times (2 \times 10^{-2}) = 4 \times 10^{-7} / \text{muon}$
- 3) Other background triggers include two hadron interactions, one of which penetrates all iron materials between the target,  $S_A$  and  $S_B$ , or multiple electromagnetic shower. All of these rates are estimated to be lower than that described in 1) or 2).

We thus estimate background dimuon trigger rates to be of the order  $10^{-6} / \text{muon}$  compared to  $\geq 5 \times 10^{-8}$  dimuon events/muon.

## II. Actions not planned in E-319

- A. The apparatus for E-319 does not require the "wide-angle muon catcher" or identifier, since deep inelastic muons detected fall within  $\theta_\mu = 150$  mrad. The ability to detect a third muon which might otherwise escape our apparatus at wide angles (up to  $18^\circ$ ) would be very useful to reduce systematic corrections to our dimuon rate. As shown in Figure 3, we plan to add a "picket fence" hodoscope at the back-side of hadron shield. These counters will be used for muon identification. In addition these counters will help us identify dimuon events with one muon scattered in the hadron shield with a low  $Q^2$  and high  $\nu$  thereby adding error to missing energy measurements.

## APPENDIX I

### E-319 Runs

E-319 has been approved for 500 hours at  $E_\mu < 300$  GeV. Our expectation is that the available muon flux at 300 GeV will be approximately  $2.5 \times 10^5$  muon/pulse. At lower energies we expect the muon flux  $\sim 10^6$ /pulse.

A brief description of four types main data runs are summarized in Table I.

1. Run I. Low  $Q^2$  triggers ( $Q^2 \leq 20 \text{ GeV}^2/c^2$ ) (50 hours)

It is necessary to run with a "thin" target located upstream so that we collect sufficient amount of data at low  $Q^2$  overlapping with kinematic regions of SLAC or E-26. This run permits also a check of acceptances and absolute normalization of data. Only a short target ( $\sim 3$  ft.) will be used for this run.

2. Data Run at  $E_\mu = 300$  GeV (Scaling Test) (250 Hours)

This is the main run for scaling tests. To select the muon energy we will have to wait until the triplet train-load is tuned. Since the  $\frac{\mu}{p}$  ratio at  $E_\mu = 300$  is approximately 1/4 of the maximum of  $2 \times 10^{-7}$  at  $E_\mu = 200$  GeV, we anticipate to run at an energy slightly lower than 300 GeV to get  $5 \times 10^5$  muons/pulse. Event rate for  $Q^2 > 20$  is  $2.6 \times 10^{-5}$ /muon and  $1.2 \times 10^{-5}$ /muon for  $Q^2 > 40 \text{ GeV}^2/c^2$ .

Configuration in #1 (Figure 1). Expected event rates are shown in Table II. for  $10^9$  muons. For comparison, yields for E203 is also quoted.

3. Data Run at  $E_\mu = 100$  GeV (Scaling Test) (120 Hours)

Since  $\frac{\mu}{p}$  at 100 GeV is expected to be twice (or more) the value at 300 GeV, the muon flux requirement will be one-half of requirement in 2) to get equal statistics for data/data comparisons.

4. Calibration Runs and Alignment Runs (~ 30 hours)

It is not clear how much time we will be able to have for these runs, but we feel that a careful energy calibration of our toroidal magnet spectrometer must be carried out before, during, and after main data runs. Small toroids (2) have been built to spread our muon beam into the active areas of the spectrometer. Data at several incident energies (5 planned: 20, 50, 100, 200, 300) will be taken. Up to 40,000 triggers per run will be recorded. Alignment runs will also be run. We shall discuss this in greater detail in Appendix II.

TABLE I

DATA RUNS	TARGET LENGTH	POSITION	NO. OF HOURS	MUON FLUX
1. 300 GeV Scaling Run	240"	Normal	250*	$2.5 \times 10^{10}$
2. 300 GeV Low $Q^2$ run	72"	"Small Angle"	30	
3. 100 GeV	240"	Normal	150**	$5 \times 10^{10}$
4. Calibration and Alignment Runs	240"	Normal	30	----

\*Assuming 10 sec per NAL pulse at  $2.5 \times 10^5$  muons/pulse

\*\* Not useful for dimuon work since  $v$  is small.

TABLE II Accepted  $Q^2$  events 300 GeV  $10^9$  Incident  $\mu$ 's

	E319 Config #1	E319 <sup>a</sup> Config #2	E319 #1 SA:SB only	E203/391 <sup>b</sup> 200 GeV
0	13396	9826	14618	-----
20	8676	8222	7406	7800
40	2530	2419	2340	3600
60	805	849	900	1700
80	307	309.63	340	880
100	159	143	161	410
120	68	55	80	190
140	28.6	22.6	38.2	82
160	13.23	9.62	21.4	33
180	4.51	3.37	8.73	13
200	1.91	1.27	4.14	4.5
220	1.01	.49	1.83	1.8
240	.25	.22	1.55	4.8
260	.11	.03	.73	
280			.11	
300				
TOTAL	25991	21862	25992	

Event rate  $Q^2 > 20$   $\frac{25992}{10^9} = 2.6 \times 10^{-5}/\mu$

Event rate  $Q^2 > 40$   $\frac{12400}{10^9} = 1.2 \times 10^{-5}/\mu$

a. Original E-319 proposal.

b. Addendum to E-203/391

APPENDIX II

E-319 Group Memo

Suggestions For Calibration and Alignment Runs

1) Calibration

We want at least the following energies:

20 GeV, 50, 100, 200, and maximum beam energy. (nominally 300).

a) Energy loss in the small magnets must be taken into account at the low energies i.e., we want 20 GeV after going through the small magnets.

b) Before taking calibration data, we must make sure that the tracks are well away from the edges of the spectrometer both at the front and at the back (e.g. 3 s.d. on the gaussian spark distributions). Otherwise we will not be able to make good fits to the gaussians.

To get 1/2% errors on the fitted means of the  $1/E'$  distributions we want

$$\frac{\Delta E'}{\sqrt{N'}} \sim 0.005$$

Using  $\frac{\Delta E'}{E'} \sim 0.12$  (it's really  $\frac{\Delta (1/E')}{(1/E')} \sim 0.12$  but this is approximate), we get

<u>E'</u>	<u>N</u>
20	480
50	1200
100	2400
200	4800
300	7200

To be safe, and to get  $< 1/2\%$  errors which is preferable, we should double the number of triggers at each energy. Since we can do  $\sim 13K/\text{hour}$  this will only take  $\sim 3-4$  hours.

If possible, one of these runs, preferably the highest energy, should accumulate a very large number of triggers. (>30-40K) so that it can be used in spark chamber alignment. This is because we will look at the data by quadrants. Remember that the highest energy is most sensitive to small misalignments.

Each of the energies should be done twice at different radii in the spectrometer (just change the current in the small toroids). This is done so that we know the reconstruction programs are radius,  $\theta$ , and B-field independent.

## 2. Energy loss

The energy loss formulae used in the Monte Carlo must be checked by measurement. No measurements of  $\mu$  energy loss have been done above 100 GeV.

We should repeat the 20, 50, 100, 200, 300 GeV calibration runs with the iron shutter closed and with similar statistics.

If we use the Al and CH<sub>2</sub> targets, we must also do runs at one energy, inserting Al and CH<sub>2</sub> in the beam to measure the energy loss in those materials.

## 3. Alignment

Aside from the calibration runs, which can be used for alignment, we should do "batwing" runs for all the "batwings" i.e. east, west, up, and down with ~ 1000 events in each.

The counters used to trigger must be small enough to avoid tracks going through the magnets.

It may also be worthwhile to degauss all the magnets and take a large number of halo triggers (50-100K) to use in alignment. If the residual field is ~ 500 gauss, a 100 GeV  $\mu$  deflects ~ 0.1 mm/toroid, so the track is practically straight. The only problem is knowing how to eliminate low energy halo.



4. Spark Chamber Efficiency

We should use a halo trigger to get single tracks more or less uniformly spaced over the spark chambers. (Data is mainly concentrated at small radius so we can't use it to find inefficiencies at large radius). This should probably be triggered once/pulse so we can keep track of chamber efficiencies as a function of time.

This trigger should probably be run at a high rate whenever the beam is too poor to take data.

CONFIG #1

Figure 1

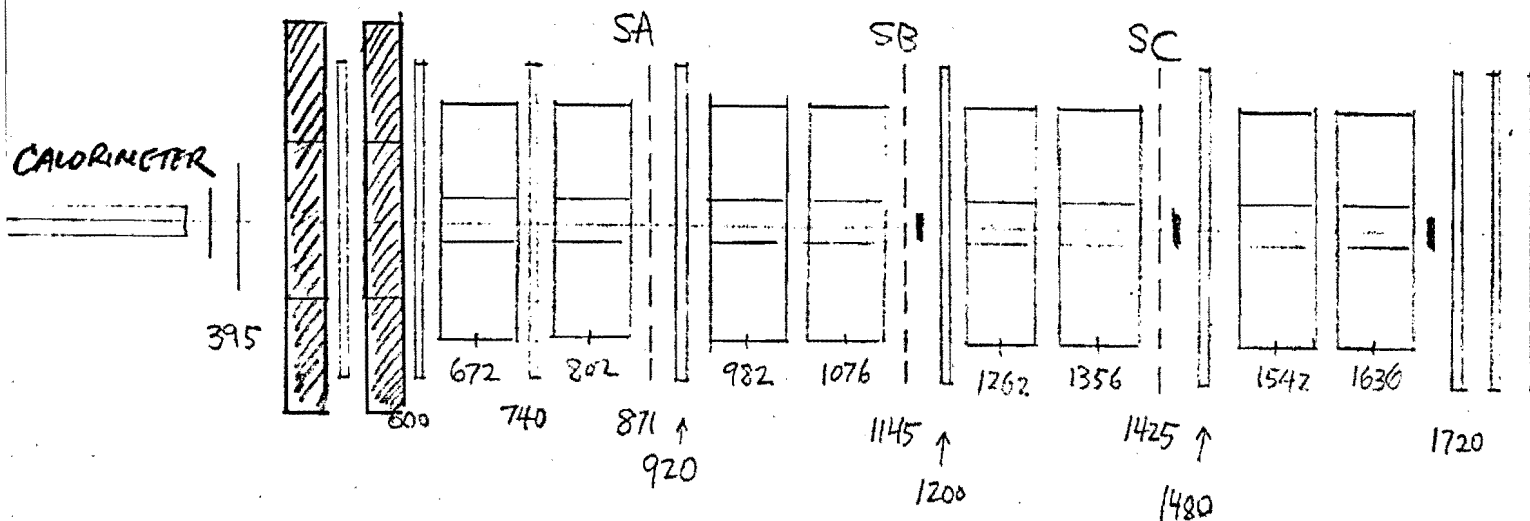
E319

CONFIGURATION

(To Be Used in E319 Actual Runs)

(Figure 3)

HADRON SHIELDS

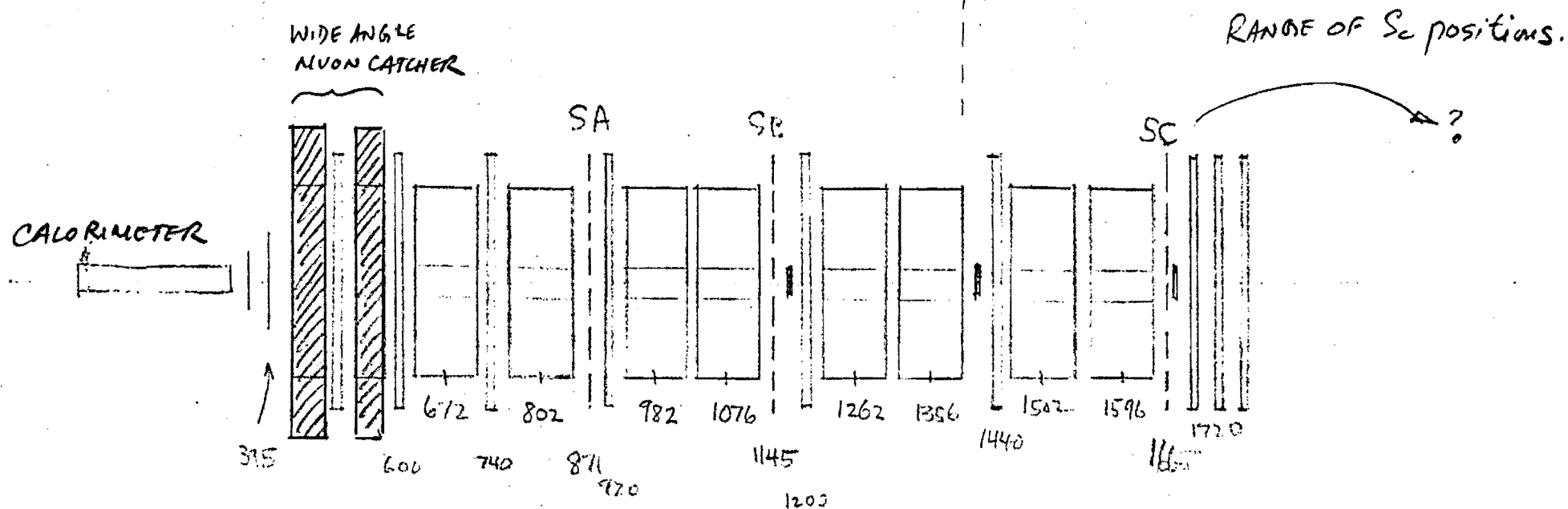


# CONFIG #2

Configuration with SC trigger bank at the end of the apparatus

# Figure 2

(DIMUON Configuration)  
For high  $P_T$  running



ZNLF 2000, 271, 1145, 1665

ZNLF 395, 600, 740, 920, 1200, 1440, 1720

SC 672 802 982 1076 1262 1356 1502 1596



# ENGINEERING NOTE

FERMILAB

SECTION  
Neutrino  
Dept.

PROJECT  
E-319  
Shield

SERIAL-CATEGORY  
76-120

PAGE  
1/1

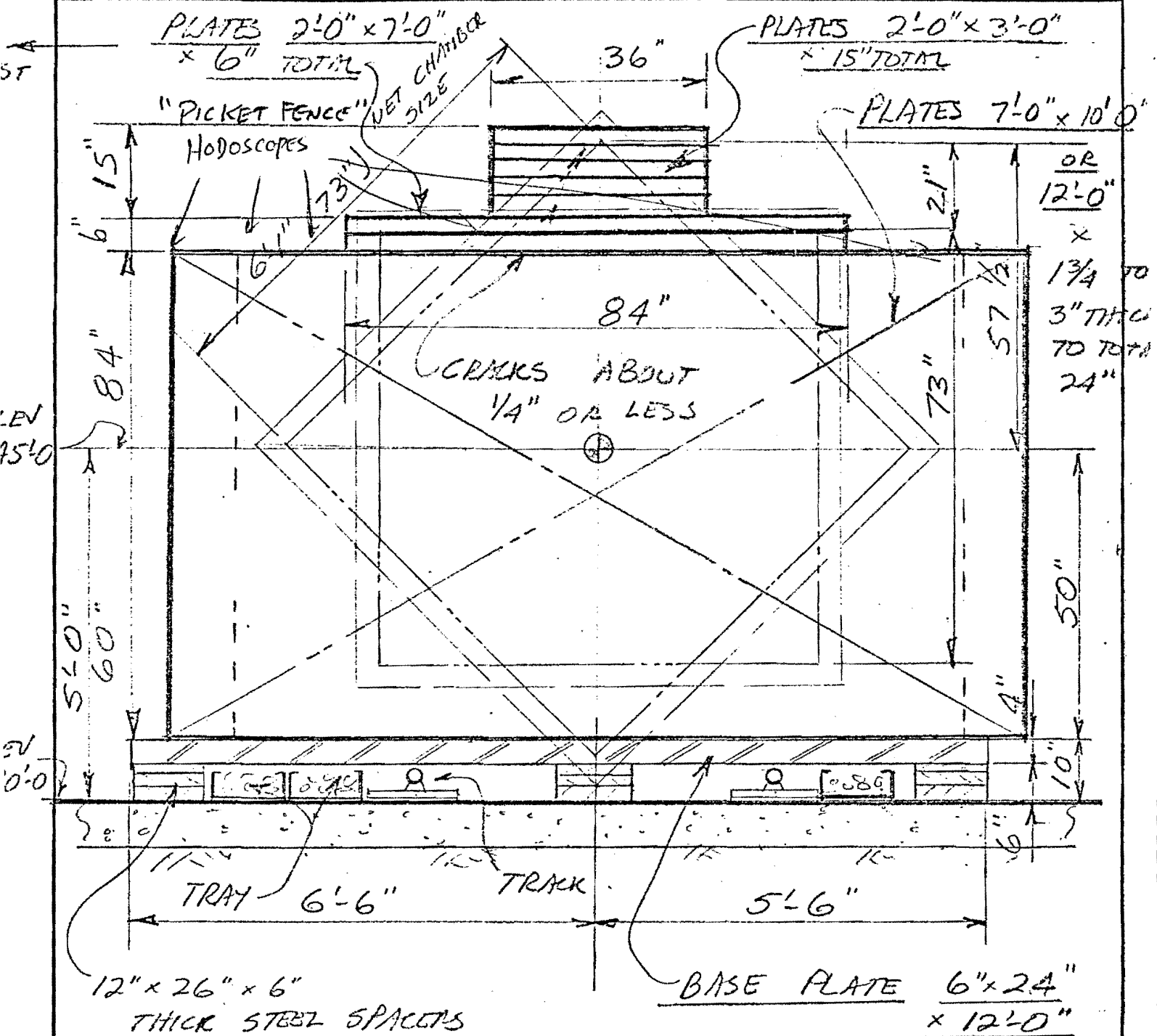
SUBJECT

HADRON SHIELD WALL E-319 (PATA)  
Typical Cross Section at Wall  
Muon Laboratory

NAME  
Wayne W. Nestander

DATE  
20 Jan. 76

REVISION DATE



3 PLACES TYPICAL SECTION

WEIGHTS - WALL SCALE 1/2" = 1'-0"

7' x 12' x 4' x 1/4" = 84 TONS LOOKING NORTH

2' x 7' x 1' x 1/4" = 4 TONS

2' x 3' x 2.5' x 1/4" = 4 TONS

TOTAL ~ 92 TONS

REQD - 2 WALLS  
24" EACH ALONG  
BEAM

PLATES - USING  
"JESSOP" STEEL -  
AISI 1060

BASE - 10

10 TONS / 100 TONS